

Design and Synthesis of Systemically Active Metabotropic Glutamate Subtype-2 and -3 (mGlu_{2/3}) Receptor Positive Allosteric Modulators (PAMs): Pharmacological Characterization and Assessment in a Rat Model of Cocaine Dependence

Raveendra-Panickar Dhanya,^{†,‡} Douglas J. Sheffler,^{†,‡} Russell Dahl,[†] Melinda Davis,[†] Pooi San Lee,[†] Li Yang,[†] Hilary Highfield Nickols,^{§,||} Hyekyung P. Cho,^{‡,||} Layton H. Smith,[†] Manoranjan S. D'Souza,[⊥] P. Jeffrey Conn,^{‡,||} Andre Der-Avakian,[⊥] Athina Markou,[⊥] and Nicholas D. P. Cosford^{*,†}

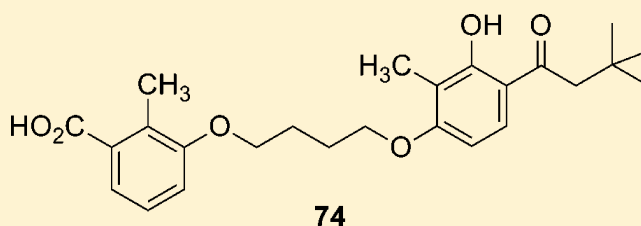
[†]Cell Death and Survival Networks Program and Conrad Prebys Center for Chemical Genomics, Sanford-Burnham Medical Research Institute, 10901 N. Torrey Pines Road, La Jolla, California 92037, United States

[‡]Department of Pharmacology, [§]Department of Pathology, and ^{||}Vanderbilt Center for Neuroscience Drug Discovery, Vanderbilt University Medical Center, Nashville, Tennessee 37232, United States

[⊥]Department of Psychiatry, School of Medicine, University of California—San Diego, La Jolla, California 92093, United States

S Supporting Information

ABSTRACT: As part of our ongoing small-molecule metabotropic glutamate (mGlu) receptor positive allosteric modulator (PAM) research, we performed structure–activity relationship (SAR) studies around a series of group II mGlu PAMs. Initial analogues exhibited weak activity as mGlu₂ receptor PAMs and no activity at mGlu₃. Compound optimization led to the identification of potent mGlu_{2/3} selective PAMs with no in vitro activity at mGlu_{1,4–8} or 45 other CNS receptors. In vitro pharmacological characterization of representative compound **44** indicated agonist-PAM activity toward mGlu₂ and PAM activity at mGlu₃. The most potent mGlu_{2/3} PAMs were characterized in assays predictive of ADME/T and pharmacokinetic (PK) properties, allowing the discovery of systemically active mGlu_{2/3} PAMs. On the basis of its overall profile, compound **74** was selected for behavioral studies and was shown to dose-dependently decrease cocaine self-administration in rats after intraperitoneal administration. These mGlu_{2/3} receptor PAMs have significant potential as small molecule tools for investigating group II mGlu pharmacology.



mGlu₂ EC₅₀ = 136 nM; Max = 96%
mGlu₃ EC₅₀ = 300 nM; Max = 109%

INTRODUCTION

Glutamate is the major excitatory neurotransmitter in the mammalian central nervous system (CNS), mediating fast synaptic transmission through ion channels, primarily the α -amino-3-hydroxy-5-methyl-4-isoxazolepropionic acid (AMPA) and kainate ionotropic glutamate receptor subtypes.¹ The metabotropic glutamate (mGlu) receptors are a family of eight G protein-coupled receptors that are activated by glutamate and perform a modulatory function in the nervous system.^{2–4} The group II mGlu receptors include the mGlu₂ and mGlu₃ receptor subtypes, which couple with G_{i/o} proteins to negatively regulate the activity of adenylyl cyclase.^{3,5} Localization studies suggest that mGlu₂ receptors act predominantly as presynaptic autoreceptors to modulate the release of glutamate into the synaptic cleft.⁶ On the other hand, mGlu₃ receptors exhibit a broad distribution in the brain and have been shown to be present on astrocytes.⁷ In addition, it has been shown that activation of mGlu₃ receptors is required for the neuroprotective effects of mGlu_{2/3} agonists toward N-methyl-D-aspartate (NMDA)

neurotoxicity in mixed cultures of astrocytes and neurons, whereas activation of mGlu₂ receptors may be harmful.⁸

Various brain regions, including the cerebral cortex, hippocampus, striatum, amygdala, frontal cortex, and nucleus accumbens, display high levels of mGlu₂ and mGlu₃ receptor binding.^{9,10} This distribution pattern suggests a role for the mGlu_{2/3} receptor subtypes in the pathology of neuropsychiatric disorders such as anxiety,¹¹ depression,^{12,13} schizophrenia,^{14,15} drug dependence,^{16–22} neuroprotection,^{23,24} Alzheimer's disease,²⁵ and sleep/wake architecture.²⁶ Thus, there is significant potential for the development of selective group II mGlu receptor activators, including agonists and positive allosteric modulators (PAMs), for the treatment of CNS diseases caused by aberrant glutamatergic signaling.

Orthosteric (glutamate site) mGlu_{2/3} agonists such as LY379268²⁷ are constrained amino acid analogues that are

Received: January 10, 2014

Published: April 15, 2014

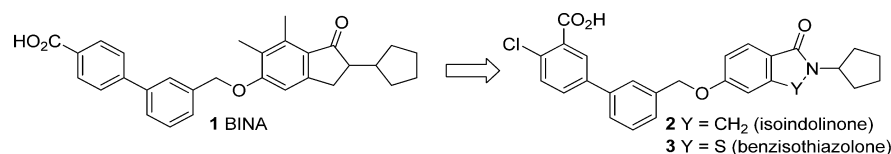


Figure 1. Structures of mGlu₂ receptor PAMs developed from BINA (1).

typically equipotent at both mGlu₂ and mGlu₃, presumably because of the high degree of sequence homology at the glutamate-binding site for these two receptors.³ Although LY541850, an orthosteric ligand with mixed mGlu₂ agonist/mGlu₃ antagonist activity, has been reported,^{28,29} currently there are no truly mGlu₂ selective orthosteric ligands available. The systemically active mGlu_{2/3} receptor agonist LY379268 has been shown to reduce glutamate release from pre-synaptic terminals in many brain regions and thus to decrease glutamatergic neurotransmission.^{30,31} LY379268 is active in several different rodent models of CNS disorders including anxiety,³² schizophrenia,³³ Huntington's disease,^{34–36} and drug dependence, where it attenuates cocaine self-administration both in rats^{20,37} and in squirrel monkeys.¹⁸ However, LY379268 also inhibits responding for food and food-seeking behavior,^{20,21,37,38} suggesting that mGlu_{2/3} receptor agonists exhibit nonselective actions on responding for drug and nondrug reinforcers.

In addition to orthosteric agonists of Group II mGlu receptors, multiple reports have recently described the synthesis and characterization of selective mGlu₂ receptor PAMs.^{5,39–46} These compounds invariably resulted from the optimization of hits obtained from high-throughput screening (HTS) of small molecule libraries. PAMs, through their interaction at allosteric sites on the mGlu receptor, positively modulate (*i.e.* potentiate) the effects of the endogenous orthosteric mGlu agonist glutamate. The advantages of PAMs compared with orthosteric agonists includes enhanced subtype selectivity, the potential for spatial and temporal modulation of receptor activation, and ease of optimization and fine-tuning of druglike properties.⁴⁷ We recently reported the design, synthesis, and in vitro and in vivo characterization of a series of potent and selective mGlu₂ receptor PAMs.^{48,49} The optimized compounds 2 and 3 (Figure 1), which were developed using the prototypical mGlu₂ receptor PAM BINA (1) as a starting point, were employed to determine the effects of selectively activating mGlu₂ receptors on cocaine or nicotine dependence.^{48,49} In these studies we showed that compound 3, unlike the mGlu_{2/3} orthosteric agonist LY379268, decreased cocaine self-administration in rats at doses that did not affect responding for food.⁴⁸ We also showed that compound 2 dose-dependently decreased nicotine self-administration in rats following oral (*po*) administration.⁴⁹ Taken together, our data suggest that mGlu₂ receptor PAMs have the potential for therapeutic utility in the treatment of drug dependence.

As noted above, there have been many accounts in the literature describing selective mGlu₂ receptor PAMs, whereas very little has been reported on compounds that potentiate the effects of glutamate at mGlu₃ receptors. This is somewhat surprising given the significant sequence homology (approximately 75%) within the transmembrane regions of mGlu₂ and mGlu₃ receptors. A single disclosure by Schann and co-workers described compound 4 (Figure 2) which was reported to be a mixed mGlu₂ receptor negative allosteric modulator (NAM)/mGlu₃ receptor PAM.⁵⁰ We hypothesized that it might be possible to design and synthesize compounds that activate both

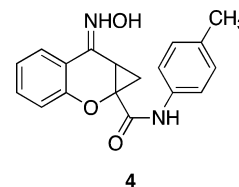


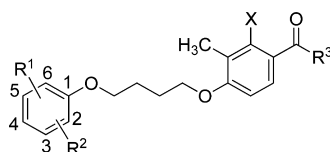
Figure 2. Structure of recently reported mGlu₂ receptor NAM/mGlu₃ receptor PAM 4.

mGlu₂ and mGlu₃ receptors through an allosteric mechanism. Considering the dearth of information on mixed mGlu_{2/3} receptor PAMs, the development of such compounds would provide valuable pharmacological tools. For example, a CNS penetrant mGlu_{2/3} receptor PAM could facilitate investigations into whether effects on food responding in rats are due to general activation of mGlu₃ receptors or an effect specific to direct activation of the mGlu receptor by agonists that act at the mGlu orthosteric binding site.

The strategy for the design and synthesis of mGlu_{2/3} receptor PAMs grew out of our general approach to the development of selective mGlu₂ receptor PAMs. In addition to exploring the structure–activity relationship (SAR) around compound 1, which led to the series of selective mGlu₂ receptor PAMs exemplified by 2 and 3,^{48,49} we also investigated compounds such as 5–7 (Figure 3). The mGlu₂ receptor PAMs 5–7 are representative of a series developed by Pinkerton and co-workers at Merck.⁵¹ The mGlu₂ receptor PAMs in this structural class were reported to exhibit varying degrees of in vitro potency and efficacy with little information provided regarding subtype selectivity. Compound 8, a selective mGlu₂ receptor PAM that bears a resemblance to compounds 5–7, was recently reported by researchers at Eli Lilly.⁵² With the exception of the optimized compound 8, most of the compounds in this series were reported to be modestly potent at mGlu₂ receptors in vitro and displayed suboptimal pharmacokinetic (PK) profiles and brain penetration in vivo. Our initial goal was to develop group II mGlu receptor PAMs having the potential for systemic activity, with a focus on maintaining or improving potency and efficacy at mGlu₂, while in parallel investigating the PAM activity at mGlu₃ receptors. Herein we describe the design, synthesis, and pharmacological characterization of a library of analogues from which a series of mixed mGlu_{2/3} receptor PAMs with unique pharmacology were discovered. Furthermore, because the selective mGlu₂ receptor PAM BINA decreased cocaine- but not food-maintained responding,³⁷ we investigated the in vivo efficacy of one of the synthesized mGlu_{2/3} receptor PAMs on cocaine- and food-maintained responding in rats.

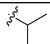
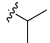
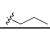
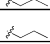
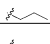
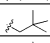
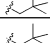
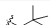
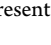
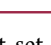
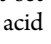
CHEMISTRY

Examination of compounds 5–7 suggested the presence of common structural elements. Specifically, they consist of an aryl ether connected via a butyl ether linker to an acetophenone derivative. Thus, we envisioned a synthetic strategy wherein the

Table 1. In Vitro Potency and Efficacy Data at mGlu₂ or mGlu₃ Receptors for PAMs^a

Cmpd ID	R ¹	R ²	X	R ³	mGlu ₂ PAM EC ₅₀ (μM)	mGlu ₂ PAM Max (%)	mGlu ₃ PAM EC ₅₀ (μM)	mGlu ₃ PAM Max (%)
4	-	-	-	-	ND	16.8 ± 1.2	ND	19.3 ± 1.7
5	4-CH ₂ CH ₂ CO ₂ H	3-OH	OH		2.449 ± 0.272	83.1 ± 3.2	ND	15.2 ± 2.7
6	4-CHCHCO-	3-O-	OH		> 10	45.2 ± 6.9	ND	27.8 ± 1.6
14	4-COOMe	H	CH ₃		ND	15.9 ± 2.4	ND	27.3 ± 2.3
15	4-COOMe	H	CH ₃		ND	14.1 ± 2.1	ND	24.2 ± 3.2
16	4-COOMe	H	OH		ND	16.4 ± 2.7	ND	22.7 ± 2.3
17	4-COOMe	H	OH		ND	12.2 ± 2.4	ND	22.0 ± 2.1
18	4-COOH	H	CH ₃		ND	19.0 ± 4.5	ND	16.6 ± 0.3
19	4-COOH	H	CH ₃		ND	16.2 ± 2.9	ND	12.2 ± 1.5
20	4-COOH	H	OH		0.122 ± 0.022	88.0 ± 1.6	2.724 ± 0.294	51.9 ± 5.8
21	4-COOH	H	OH		0.824 ± 0.071	82.6 ± 1.0	> 10	26.7 ± 1.7
22	3-COOH	H	CH ₃		ND	12.1 ± 2.5	ND	18.3 ± 1.9
23	3-COOH	H	CH ₃		ND	22.4 ± 6.7	ND	16.5 ± 1.2
24	3-COOH	H	OH		0.222 ± 0.031	84.5 ± 3.0	1.434 ± 0.136	69.9 ± 4.5
25	3-COOH	H	OH		0.451 ± 0.035	80.6 ± 2.8	3.400 ± 0.783	92.9 ± 8.9
26	2-COOH	H	CH ₃		0.976 ± 0.041	76.2 ± 6.3	ND	30.7 ± 2.3
27	2-COOH	H	CH ₃		2.581 ± 0.157	67.1 ± 7.2	ND	28.0 ± 3.1
28	2-COOH	H	OH		0.415 ± 0.070	92.4 ± 9.6	ND	28.1 ± 3.2
29	2-COOH	H	OH		0.335 ± 0.028	98.8 ± 8.0	ND	32.9 ± 3.3
30	4-COOH	3-Cl	CH ₃		> 10	33.1 ± 7.0	ND	12.0 ± 3.9
31	4-COOH	3-Cl	CH ₃		2.415 ± 0.188	61.8 ± 8.3	> 10	35.5 ± 1.1
32	4-COOH	3-Cl	OH		0.151 ± 0.006	80.5 ± 1.1	2.048 ± 0.289	49.5 ± 2.6
33	4-COOH	3-Cl	OH		0.510 ± 0.057	80.8 ± 2.4	2.247 ± 0.081	40.0 ± 4.8
34	3-COOH	4-F	CH ₃		ND	15.8 ± 4.1	ND	13.8 ± 3.1
35	3-COOH	4-F	CH ₃		ND	14.6 ± 2.8	ND	12.6 ± 1.5
36	3-COOH	4-F	OH		0.153 ± 0.010	84.5 ± 1.2	0.920 ± 0.071	81.7 ± 4.2
37	3-COOH	4-F	OH		0.699 ± 0.121	81.0 ± 2.8	2.492 ± 0.401	98.4 ± 9.9
38	5-COOH	2-CH ₃	OH		0.454 ± 0.054	76.9 ± 5.5	>10	29.4 ± 2.8
39	5-COOH	2-CH ₃	OH		1.290 ± 0.265	67.5 ± 4.7	>10	26.9 ± 2.4
40	3-COOH	2-CH ₃	OH		0.192 ± 0.017	83.9 ± 3.2	1.853 ± 0.356	42.1 ± 4.1
41	3-COOH	2-CH ₃	OH		0.608 ± 0.039	84.6 ± 4.4	>10	28.4 ± 2.3
42	4-COOH	2-F	OH		0.102 ± 0.015	85.0 ± 2.5	1.417 ± 0.061	67.7 ± 4.3
43	4-COOH	2-F	OH		0.639 ± 0.054	83.8 ± 3.9	>10	31.2 ± 2.3
44	4-COOH	2-OMe	OH		0.040 ± 0.006	85.7 ± 2.5	0.614 ± 0.098	73.9 ± 6.0
45	4-COOH	2-OMe	OH		0.228 ± 0.046	95.4 ± 2.7	1.905 ± 1.131	46.9 ± 6.2
46	4-COOH	2-Cl	OH		0.096 ± 0.020	99.5 ± 0.9	1.140 ± 0.010	62.9 ± 2.4
47	4-COOH	2-Cl	OH		0.237 ± 0.006	82.2 ± 3.4	>10	27.4 ± 2.3
48	4-COOH	3-CH ₃	OH		0.173 ± 0.038	93.3 ± 1.5	3.907 ± 1.972	41.9 ± 4.0
49	4-COOH	3-CH ₃	OH		0.564 ± 0.039	83.6 ± 2.5	>10	23.7 ± 2.6
50	5-COOH	2-OMe	OH		0.155 ± 0.029	89.7 ± 1.7	0.737 ± 0.085	100.1 ± 5.2
51	5-COOH	2-OMe	OH		0.425 ± 0.078	91.8 ± 2.8	1.021 ± 0.091	67.6 ± 1.5
52	4-COOH	2-OMe	OH		0.161 ± 0.075	86.3 ± 1.1	ND	26.3 ± 2.2
53	5-COOH	2-OMe	OH		1.091 ± 0.048	70.7 ± 8.5	ND	34.8 ± 3.1
54	3-COOH	2-CH ₃	OH		0.200 ± 0.050	79.2 ± 2.4	ND	17.1 ± 8.0
55	3-COOH	4-F	OH		0.259 ± 0.084	75.5 ± 6.1	ND	16.8 ± 7.3
56	4-COOH	2-CH ₃	OH		0.050 ± 0.012	83.1 ± 4.3	ND	25.4 ± 5.2
57	4-COOH	2-OMe	OH		0.114 ± 0.054	86.5 ± 1.1	ND	25.9 ± 6.2
58	5-COOH	2-OMe	OH		0.162 ± 0.055	72.6 ± 7.5	6.359 ± 3.655	62.5 ± 5.3
59	3-COOH	2-CH ₃	OH		0.062 ± 0.011	71.3 ± 6.7	ND	16.3 ± 6.0
60	3-COOH	4-F	OH		0.124 ± 0.020	66.6 ± 5.3	ND	18.4 ± 4.5
61	4-COOH	2-CH ₃	OH		0.082 ± 0.016	86.6 ± 6.0	ND	22.7 ± 5.6
62	4-COOH	2-OMe	OH		0.113 ± 0.046	73.1 ± 6.9	ND	25.6 ± 3.8
63	5-COOH	2-OMe	OH		0.116 ± 0.024	66.6 ± 2.3	0.588 ± 0.104	59.9 ± 1.8
64	3-COOH	2-CH ₃	OH		0.149 ± 0.056	66.9 ± 2.1	ND	27.1 ± 1.6

Table 1. continued

Cmpd ID	R ¹	R ²	X	R ³	mGlu ₂ PAM EC ₅₀ (μM)	mGlu ₂ PAM Max (%)	mGlu ₃ PAM EC ₅₀ (μM)	mGlu ₃ PAM Max (%)
65	3-COOH	4-F	OH		0.171 ± 0.029	74.1 ± 2.1	>10	31.3 ± 6.5
66	4-COOH	2-CH ₃	OH		0.234 ± 0.030	76.9 ± 3.2	ND	25.2 ± 8.8
67	4-COOH	2-OMe	OH		0.034 ± 0.004	85.5 ± 0.6	1.830 ± 0.380	61.9 ± 3.8
68	5-COOH	2-OMe	OH		0.103 ± 0.026	82.8 ± 4.8	0.496 ± 0.076	64.2 ± 3.2
69	3-COOH	2-CH ₃	OH		0.052 ± 0.025	82.4 ± 6.4	> 10	53.0 ± 3.9
70	3-COOH	4-F	OH		0.074 ± 0.014	87.5 ± 2.4	0.438 ± 0.020	56.9 ± 3.9
71	4-COOH	2-CH ₃	OH		0.104 ± 0.014	79.3 ± 6.0	> 10	40.5 ± 7.8
72	5-COOH	2-OMe	OH		0.184 ± 0.033	96.0 ± 2.2	0.151 ± 0.028	105.5 ± 2.9
73	4-COOH	2-OMe	OH		0.047 ± 0.009	98.6 ± 4.7	0.310 ± 0.029	109.4 ± 1.8
74	3-COOH	2-Me	OH		0.136 ± 0.032	95.8 ± 3.5	0.300 ± 0.054	108.8 ± 2.3
75	3-COOH	4-F	OH		0.208 ± 0.036	94.6 ± 2.1	0.258 ± 0.063	101.7 ± 4.1

^amGlu₂ PAM EC₅₀ (μM) data and glutamate Max (%) data represent the mean ± SEM for at least three independent experiments performed in triplicate. ND = not determined.

These results prompted us to synthesize and test the next set of analogues (compounds 30–51) containing carboxylic acid moieties at the 3- or 4-position (R¹) in addition to substituents at other positions around the aryl ether ring (i.e., R² = F, Cl, Me, or OMe). In this series, the analogues containing X = Me (30, 31, 34, 35) continued the trend of very weak (31, EC₅₀ > 10 μM, 36% efficacy) or no mGlu₃ activity (30, 34, 35, 12%–14% efficacy), and therefore, all subsequent analogues were synthesized with X = OH. Furthermore, several of the analogues in this group (39, 41, 43, 47, and 49) were active as PAMs at mGlu₂ but were essentially inactive at mGlu₃ receptors (24%–31% efficacy). However, in addition to being submicromolar PAMs at mGlu₂, compounds 32, 33, 37, 40, 42, 45, 46, 48, and 51 were active as PAMs at mGlu₃ receptors in the micromolar range (EC₅₀ ≈ 1–4 μM, 40%–98% efficacy). Most promising of all, compounds 36, 44, and 50 possessed submicromolar PAM activity at mGlu₃ receptors as well as good potency at mGlu₂. Especially noteworthy were compounds 44 and 50, with EC₅₀ values in the 600–700 nM range at mGlu₃ with excellent efficacy as PAMs (74% and 100%, respectively). These results suggested that our goal of producing PAMs with potent activity at both mGlu₂ and mGlu₃ receptors was attainable. Having identified favorable substitution patterns for the left-hand aryl ether moiety, we next designed a series of analogues (compounds 52–75) to investigate which ketone alkyl group (R³) would impart the best potency and efficacy at both mGlu₂ and mGlu₃ receptors. Thus, in this set of analogues, compounds were synthesized with R³ = methyl (52–56), ethyl (57–61), isopropyl (62–66), *n*-propyl (67–71), or *tert*-butylmethylene (72–75). Interestingly, none of the methyl ketone derivatives (52–56) had activity at mGlu₃ receptors, while in the ethyl ketone series (57–61) only compound 58 (5-CO₂H, 2-OMe) had activity at mGlu₃ (EC₅₀ = 6359 nM, 63% efficacy). In the isopropyl ketone series, only compound 63 (5-CO₂H, 2-OMe) had activity at mGlu₃ (EC₅₀ = 588 nM, 60% efficacy). On the other hand, in the *n*-propyl series, all compounds demonstrated some level of activity. While 69 and 71 were weakly active at mGlu₃ (EC₅₀s > 10 μM, 53% and 41% efficacy, respectively), 67 (4-CO₂H, 2-OMe), 68 (5-CO₂H, 2-OMe), and 70 (3-CO₂H, 4-F) demonstrated more potent mGlu₃ activity (EC₅₀ = 1830 nM, 62% efficacy, EC₅₀ = 496 nM, 64% efficacy, EC₅₀ = 438 nM, 57% efficacy, respectively). It is noteworthy that compound 67

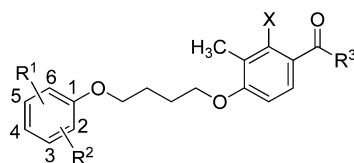
(4-CO₂H, 2-OMe) was the most potent PAM and selective for mGlu₂ with good efficacy (EC₅₀ = 34 nM, 86% efficacy). Finally, in the *tert*-butylmethylene series (compounds 72–75) all four analogues exhibited good potency and excellent efficacy for both mGlu₂ and mGlu₃ receptors. Compound 72 was the most potent against mGlu₃ (EC₅₀ = 151 nM, 106% efficacy) with similar potency against mGlu₂, while compounds 73–75 fell into the 258–310 nM potency range (102%–110% efficacy) against mGlu₃ receptors. Thus, a combination of favored left-hand aryl ether moieties with R³ = *tert*-butylmethylene provides compounds with unique PAM activity at both mGlu₂ and mGlu₃ receptors.

With these results in hand, we tested some of the most promising new PAMs to provide an estimation of their druglike properties in vitro using absorption, distribution, metabolism, and excretion (ADME) assays. The results of these studies are shown in Table 2. The permeability across artificial membranes was assessed via the parallel artificial membrane permeability assay (PAMPA) assay and showed a range of results, with most compounds showing some degree of permeability. Plasma and microsomal stability was likewise acceptable, with only four of the analogues showing less than 20% remaining after 1 h. In addition, an algorithm was used to provide an estimate of plasma protein binding for 11 of the analogues. The data, which are provided in the Supporting Information (Table S1), suggest that the compounds in this series are all >90% plasma protein bound.

Compounds 20, 25, 33, 44, 67, 72, and 73 were profiled against the remaining mGlu receptor subtypes to determine their selectivity relative to mGlu₂ and mGlu₃ (Table 3). With the exception of 67, which displayed weak antagonist/NAM activity (IC₅₀ > 10 μM) at mGlu₁ and mGlu₄, and compound 73, which showed weak PAM activity at mGlu₆ (EC₅₀ > 10 μM), these compounds were found to be highly selective for mGlu₂ and mGlu₃. As a representative of this series, compound 72 was profiled against a representative panel of CNS receptors through the NIMH Psychoactive Drug Screening Program (PDSP; see <http://pdsp.med.unc.edu/indexR.html> for details). As shown in Table S2 (see Supporting Information), at 10 μM, no binding activity was detected for compound 72 at 45 CNS receptors, suggesting that the new mGlu_{2/3} PAMs have a low likelihood of off-target activity.

At a relatively early stage of the project and on the basis of the overall in vitro profile of the PAMs (Tables 1 and 2),

Table 2. In Vitro ADME Data for Group II mGlu PAMs



Cmpd ID	R ¹	R ²	X	R ³	PAMPA (LogPapp) ^a	Plasma Stability ^b	Microsomal stability ^c
20	4-COOH	H	OH		-5.17	95	66
22	3-COOH	H	CH ₃		-5.47	106	29
24	3-COOH	H	OH		-5.19	100	51
25	3-COOH	H	OH		-4.99	99	55
26	2-COOH	H	CH ₃		-4.69	99	9
33	4-COOH	3-Cl	OH		-5.33	97	67
36	3-COOH	4-F	OH		-5.43	101	59
38	3-COOH	2-CH ₃	OH		-7.94	96	21
39	3-COOH	2-CH ₃	OH		-6.73	100	9
40	3-COOH	2-CH ₃	OH		-4.92	100	41
41	3-COOH	2-CH ₃	OH		-6.54	99	59
42	4-COOH	2-F	OH		-7.18	106	57
43	4-COOH	2-F	OH		-5.93	97	66
44	4-COOH	2-OMe	OH		-6.36	99	43
45	4-COOH	2-OMe	OH		-6.54	100	31
46	4-COOH	2-Cl	OH		-7.94	123	61
47	4-COOH	2-Cl	OH		-8.54	120	21
48	4-COOH	3-CH ₃	OH		-8.24	101	57
49	4-COOH	3-CH ₃	OH		-6.82	114	55
50	5-COOH	2-OMe	OH		-6.12	99	5
51	5-COOH	2-OMe	OH		-7.28	103	14
60	3-COOH	4-F	OH		-5.12	96	35
65	3-COOH	4-F	OH		-5.30	83	60
68	5-COOH	2-OMe	OH		-5.24	78	1
72	5-COOH	2-OMe	OH		-5.42	63	39
73	4-COOH	2-OMe	OH		-5.46	48	49
74	3-COOH	2-Me	OH		-5.63	89	51
75	3-COOH	4-F	OH		-5.66	83	58

^aPermeability is monitored by measuring the amount of compound that can diffuse through a polar brain lipid membrane to predict BBB permeability.⁴² ^bPercent remaining after incubation for 60 min at 37.5 °C.

we selected compounds **20**, **36**, **44**, and **50** for in vivo assessment of pharmacokinetic (PK) properties in rats. For this initial evaluation we determined the PK properties of the compounds by oral (po) and intravenous (iv) routes of administration as shown in Tables 4 and 5, respectively. The PAMs were found to be systemically bioavailable with half-life ($t_{1/2}$) values of greater than 90 min when dosed po and demonstrate a range of maximal plasma levels from a low of 1.05 μ M (**50**) to a high of 12.46 μ M (**36**) (Table 4). All compounds had moderate volume of distribution at steady state (V_{dss}) and medium to high clearance (CL) values, indicating moderate metabolism with a primary distribution in plasma and extracellular fluids, suggesting that one or more of the PAMs might have promise as candidates for in vivo studies (Table 5). The four compounds exhibited low (**20**) to good oral bioavailability (**50**) (% F) albeit at the relatively high oral dose of 20 mg/kg; however, the brain levels of **20**, **36**, and **44** were low, resulting in low brain/plasma ratios. Although the brain/plasma ratios of these compounds are low, the total brain concentrations of **20** and **44** are 9-fold and 18-fold above the in vitro EC_{50} for mGlu₂, respectively, and close to the in vitro EC_{50} s for mGlu₃.

Since compound **44** had shown the best mix of in vitro and in vivo properties at this stage, including potent activity and efficacy at mGlu₃ receptors, this PAM was selected for comprehensive in vitro pharmacological characterization. We began with a more detailed investigation of the activity of **44** in the mGlu₂ and mGlu₃ GIRK thallium flux assays. The nature of the GIRK assay requires that each compound is screened for a single mode of pharmacology at a time, since activity is only detected through the GIRK channel when thallium is added to the assay. The data presented in Table 1 represent compounds screened for activity in "PAM mode", where a test compound is added, followed 2.5 min later by an EC_{20} concentration of glutamate in the presence of thallium. We had noted that the response of **44** in "PAM mode" toward mGlu₂ decreased slightly at higher concentrations of test compound (Figure 4A). This decrease could be caused by either receptor desensitization or intrinsic agonist activity of **44** that was not detected because of the mode in which the functional assay was performed. To investigate this further, we carried out the same experiments in the absence of an EC_{20} concentration of agonist (agonist mode). For these experiments, test compounds were

Table 3. mGlu Receptor Subtype Selectivity^a

	compound						
	20	25	33	44	67	72	73
mGlu ₁	inactive ^b	inactive ^b	inactive ^b	inactive ^b	antagonist FS = 0.3 <i>E</i> _{min} = 3% <i>E</i> _{max} = 79%	inactive ^b	inactive ^b
mGlu ₂	Ago-PAM FS = 3.2 <i>E</i> _{min} = 54% <i>E</i> _{max} = 77%	Ago-PAM FS = 12.5 <i>E</i> _{min} = 45% <i>E</i> _{max} = 71%	Ago-PAM FS = 13.3 <i>E</i> _{min} = 54% <i>E</i> _{max} = 77%	Ago-PAM FS = ND <i>E</i> _{min} = 90% <i>E</i> _{max} = 95%	Ago-PAM FS = ND <i>E</i> _{min} = 79% <i>E</i> _{max} = 92%	Ago-PAM FS = ND <i>E</i> _{min} = 72% <i>E</i> _{max} = 95%	Ago-PAM FS = ND <i>E</i> _{min} = 79% <i>E</i> _{max} = 92%
mGlu ₃	PAM FS = 2.7 <i>E</i> _{min} = 9% <i>E</i> _{max} = 153%	PAM FS = 4.5 <i>E</i> _{min} = 6% <i>E</i> _{max} = 143%	PAM FS = 2.5 <i>E</i> _{min} = 10% <i>E</i> _{max} = 143%	PAM FS = 3.9 <i>E</i> _{min} = 4% <i>E</i> _{max} = 116%	PAM FS = 2.9 <i>E</i> _{min} = 1% <i>E</i> _{max} = 88%	Ago-PAM FS = 7.1 <i>E</i> _{min} = 54% <i>E</i> _{max} = 95%	Ago-PAM FS = 8.9 <i>E</i> _{min} = 30% <i>E</i> _{max} = 99%
mGlu ₄	inactive ^b	inactive ^b	inactive ^b	inactive ^b	antagonist FS = 1.9 <i>E</i> _{min} = 0% <i>E</i> _{max} = 74%	inactive ^b	inactive ^b
mGlu ₅	inactive ^b	inactive ^b	inactive ^b	inactive ^b	inactive ^b	inactive ^b	inactive ^b
mGlu ₆	inactive ^b	inactive ^b	inactive ^b	inactive ^b	inactive ^b	inactive ^b	PAM FS = 2.0 <i>E</i> _{min} = 8% <i>E</i> _{max} = 93%
mGlu ₇	inactive ^b	inactive ^b	inactive ^b	inactive ^b	inactive ^b	inactive ^b	inactive ^b
mGlu ₈	inactive ^b	inactive ^b	inactive ^b	inactive ^b	inactive ^b	inactive ^b	inactive ^b

^aIn these selectivity experiments, for all receptors a full concentration–response of agonist was performed once in triplicate in the presence and absence of a 10 μ M final concentration of each compound. This allows determination of positive allosteric modulator (PAM) (left shift of the agonist concentration response curve), antagonist (right shift in the agonist concentration response with a possible decrease in maximal agonist response), and agonist (increase in baseline response) activity in a single experiment. General activity for each compound at each mGlu is listed (PAM, antagonist, Ago-PAM, inactive) followed by the fold-shift (FS) of the agonist concentration–response obtained. Where tested compounds demonstrate activity toward an mGlu receptor subtype, the maximal (*E*_{max}) and minimal (*E*_{min}) responses of the concentration–response of agonist are indicated. Where 10 μ M test compound induced greater than a 2-fold shift (FS) of the glutamate concentration–response curve (L-AP4 in the case of mGlu₇), full compound concentration–response curves were performed in triplicate on 3 different days to assess compound potency. Compound 67 showed weak antagonist/NAM activity (IC₅₀ > 10 μ M) at mGlu₁ and mGlu₄, and compound 73 showed weak PAM activity at mGlu₆ (EC₅₀ > 10 μ M). ^bInactive compounds show no ability to left- or right-shift the agonist concentration response curve at 10 μ M. ND = not determined.

Table 4. In Vivo PK Data for mGlu₂/mGlu₃ PAMs in Rats after po Administration (20 mg/kg)^a

compd	<i>C</i> _{max} (μ M)	<i>T</i> _{max} (min)	AUC _(0–t) (μ mol/L)·min	<i>T</i> _{1/2} (min)	<i>F</i> (%)	brain (μ M)	plasma (μ M)	brain/plasma
20	2.57 ± 0.45	135 ± 15	544.8 ± 75.4	303 ± 55	23.5	1.12 ± 0.43	5.29 ± 1.98	0.20 ± 0.03
36	12.46 ± 6.42	30 ± 0	720.5 ± 283.4	89 ± 17	58.2	0.23 ± 0.06	4.23 ± 1.19	0.06 ± 0.03
44	2.75 ± 0.47	90 ± 17	1274.6 ± 246.3	471 ± 89	41.9	0.81 ± 0.17	16.38 ± 1.13	0.05 ± 0.01
50	1.05 ± 0.15	96 ± 40	466.2 ± 105.2	569 ± 199	60.4	ND	ND	ND

^a*C*_{max}: maximum concentration of the compound detected in plasma. *T*_{max}: time at *C*_{max}. AUC: area under the curve. *t*_{1/2}: terminal half-life. *F*: oral bioavailability. Brains and plasma were harvested at or near the *T*_{max}. Compounds were dosed in a volume of 2 mL/kg po (*n* = 3–4) at 20 mg/kg in 0.6% Tween 80. ND = not determined.

added in the presence of thallium and GIRK activity was immediately monitored. We found that 44 displayed intrinsic agonist activity toward mGlu₂ but not mGlu₃ in the GIRK assay (Figure 4B). Thus, this compound is best characterized as having mGlu₂ agonist-PAM activity and mGlu₃ PAM activity in the GIRK thallium flux assays.

We next evaluated 44 in a fold-shift assay, another measure of the potentiating activity of a PAM toward the orthosteric

ligand glutamate (Figure 5). Fold-shift values are calculated by determining the ratio of the potency of the orthosteric agonist glutamate in the presence and absence of increasing concentrations of an allosteric modulator. Increasing fixed concentrations of 44 dose-dependently shifted the glutamate concentration–response of mGlu₂ (Figure 5A) and mGlu₃ (Figure 5B) to the left, consistent with an enhancement of glutamate responses. For these assays, the Ago-PAM activity

Table 5. In Vivo PK Data for mGlu₂/mGlu₃ PAMs in Rats after iv Administration (2 mg/kg)^a

compd	C _{max} (μM)	CL (mL·min ⁻¹ ·kg ⁻¹)	Vd _{ss} (L·kg ⁻¹)	AUC _(0→t) (μmol/L)·min	T _{1/2} (min)
20	5.00 ± 0.60	21.09 ± 3.66	0.81 ± 0.14	231.7 ± 42.12	30 ± 2
36	3.52 ± 0.13	38.78 ± 2.55	0.89 ± 0.03	123.7 ± 7.7	18 ± 3
44	6.43 ± 0.39	14.58 ± 1.18	0.55 ± 0.04	304.6 ± 25.8	28 ± 0
50	2.15 ± 0.14	58.29 ± 7.98	2.87 ± 0.60	77.2 ± 8.0	57 ± 12

^aC_{max}: maximum concentration of the compound detected in plasma. AUC: area under the curve. t_{1/2}: terminal half-life. CL: clearance. Vd_{ss}: steady state volume of distribution. Compounds were injected in a volume of 1 mL/kg iv (n = 3–4) through an iv catheter at 2 mg/kg in 0.6% Tween 80 or in 1 M NaOH. pH was adjusted to ~7.

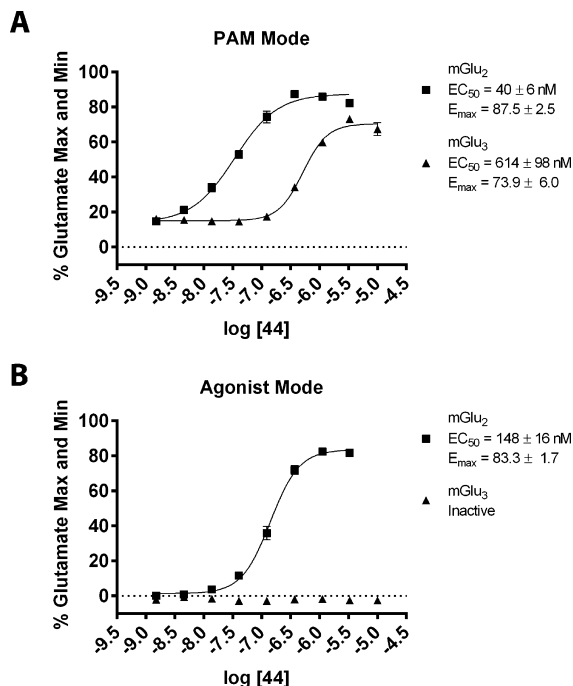


Figure 4. Compound 44 displays Ago-PAM activity toward mGlu₂ and PAM activity toward mGlu₃ in GIRK thallium-flux assays. A concentration–response of 44 was performed in the presence (A) and absence (B) of an EC₂₀ of glutamate in either the mGlu₂ GIRK assay (squares) or mGlu₃ GIRK assay (triangles). In the mGlu₂ assay, 44 displays both agonist and PAM activity and is characterized as an Ago-PAM. In the mGlu₃ assay, only PAM activity is detected. Data were analyzed using nonlinear regression, providing EC₅₀ values for each curve. Data were obtained from three separate experiments performed in triplicate, normalized to the response to 100 μM glutamate in each experiment, and are expressed as the mean ± SEM.

toward mGlu₂ is readily apparent as the increase in baseline at low concentrations of glutamate (Figure 5A). These data are in contrast with the results for mGlu₃ (Figure 5B), which does not show a change in baseline of the glutamate dose–response.

In the final set of pharmacological characterization experiments, we evaluated the potent PAM 44 in an orthogonal assay of mGlu₃ and mGlu₂ activity. For mGlu₃ we utilized the TREx tetracycline-inducible system (Invitrogen). We developed a cell line in which the expression of mGlu₃ is dose-dependently induced by tetracycline (Tet) and functionally coupled to calcium mobilization by the promiscuous G protein G_{α15} (Figure 6). In the absence of Tet, no measurable expression of mGlu₃ is detected either by Western blot (Figure 6A) or by functional response to calcium mobilization (Figure 6B). The optimal calcium mobilization response for this cell line was achieved at 20 ng/mL Tet for 20 h prior to assay. This concentration of Tet was then utilized for further characterization of 44 in the

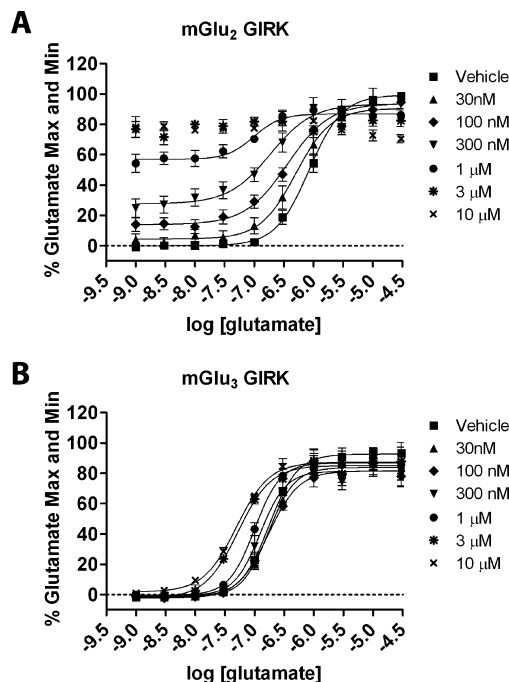


Figure 5. Compound 44 dose-dependently induces a leftward shift in the glutamate concentration response at (A) mGlu₂ and (B) mGlu₃ in GIRK thallium flux assays. The increase in baseline in the mGlu₂ GIRK assay at higher concentrations of 44 is due to the Ago-PAM activity of this compound. The leftward shifts induced by 44 indicate a potentiation of the response of mGlu₂ and mGlu₃ to glutamate. The maximal fold-shift at mGlu₂ is 4.50 ± 0.96 and was derived from the test concentration of 44 (300 nM) due to Ago-PAM activity. The maximal fold-shift at mGlu₃ is 5.48 ± 0.27 for the 10 μM test concentration. Concentration–response relationships were generated by adding a fixed concentration of 44 to cells as indicated, followed by increasing concentrations of glutamate. Data were analyzed using nonlinear regression, providing EC₅₀ values for each curve. Data were obtained from three separate experiments performed in duplicate, normalized to the response to 100 μM glutamate in each experiment, and are expressed as the mean ± SEM.

TREx293 mGlu₃ G_{α15} calcium assay (Figure 7B), which shows that 44 demonstrates mGlu₃ PAM activity in this orthogonal assay whereas the mGlu₂ selective PAM BINA remains inactive. These compounds were also evaluated in calcium assays utilizing HEK293A mGlu₂ G_{α15} cells as shown in Figure 7A. Unlike the mGlu₂ GIRK assay where it displays Ago-PAM activity, compound 44 behaves as a PAM in the calcium assay. In future experiments, it will be essential to determine the potency and selectivity of 44 in native tissue preparations to determine whether the observed profile in vitro is replicated in vivo.

Following the in vitro pharmacological characterization of 44 as a representative analogue of this class of mGlu_{2/3} PAMs, we wished to evaluate a member of this series in efficacy studies

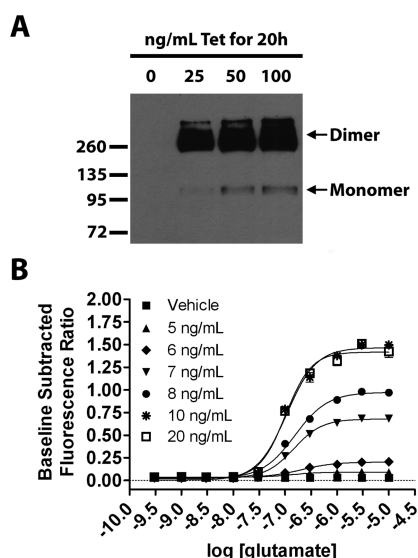


Figure 6. Development of a cell line with inducible mGlu₃ expression coupled to calcium mobilization via the promiscuous G protein G_{α15}. (A) TEx293 mGlu₃ G_{α15} cells were stimulated with the indicated concentrations of tetracycline (Tet) for 20 h. Protein lysates were prepared. Equivalent amounts of protein were loaded for all lanes, and mGlu_{2/3} expression was detected by Western blot. Both monomeric and dimeric mGlu₃ were detected as indicated. (B) TEx293 mGlu₃ G_{α15} cells were stimulated with the indicated concentrations of Tet for 20 h, and a calcium mobilization assay was performed. Tet dose-dependently induced a glutamate-stimulated calcium response that was maximal at 20 ng/mL Tet. Data were analyzed using nonlinear regression. Data were obtained from three separate experiments performed in triplicate, normalized to the response to 100 μ M glutamate in each experiment, and are expressed as the mean \pm SEM.

in rats. Given the low brain levels achieved by po dosing for compounds **20**, **36**, **44**, and **50** (Table 4), we evaluated nine compounds by intraperitoneal (ip) dosing in order to avoid first pass metabolism and to cast a wider net for a compound suitable for rat efficacy studies (Table 6). All compound plasma levels were determined, but only those with the highest plasma concentrations (i.e., **44**, **73**, **74**, and **75**) were evaluated for brain levels. On the basis of its combination of potency, selectivity, and PK properties, compound **74** was selected for efficacy studies in rats.

Taking all the relevant data into account, we determined that the mGlu_{2/3} receptor PAM **74** would be a good candidate for evaluation in a rat model of cocaine dependence. When assessed in vivo, compound **74** dose-dependently decreased cocaine- and food-maintained responding [compound **74** dose main effect: $F_{3,51} = 14.55$; $p < 0.0001$] (Figure 8). Interestingly, however, cocaine-maintained responding was decreased to a greater extent than food-maintained responding at the highest dose tested (40 mg/kg; $p < 0.05$). Because of the within-subjects design of the dose response (i.e., each rat received each dose of compound **74** using a Latin-square design), it was not possible to collect brain samples to determine brain concentrations of compound **74** at 40 mg/kg during behavioral testing. It is unlikely that brain concentrations of compound **74** differed between cocaine- and food-maintained rats at this dose, suggesting that the observed differences in behavior were not a function of group differences in brain pharmacokinetic properties of compound **74**, although this should be confirmed in future studies. We have previously shown that the mGlu_{2/3} receptor agonist LY379268 similarly decreased both cocaine-

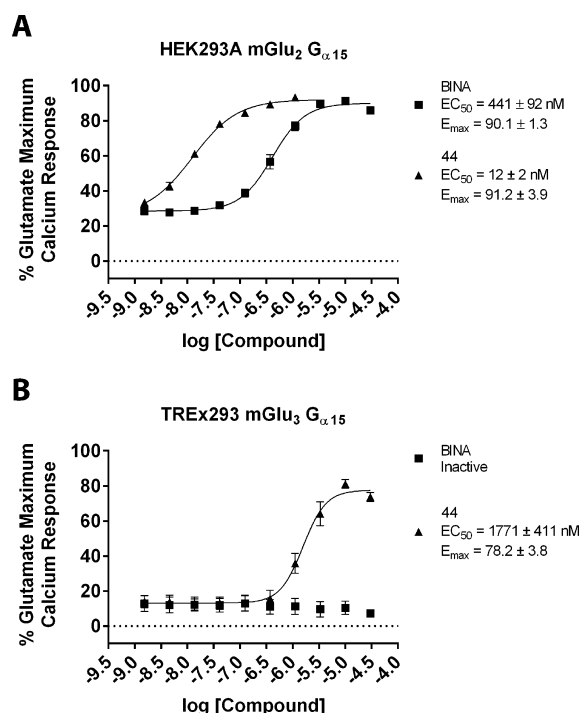


Figure 7. Compound **44** displays PAM activity toward mGlu₂ and mGlu₃ in calcium assays utilizing the promiscuous G protein G_{α15}. A concentration–response of **44** (triangles) and the control mGlu₂ selective PAM BINA (squares) was performed in the presence of an EC₂₀ of glutamate in either the (A) HEK293A mGlu₂ G_{α15} calcium assay or (B) TEx293 mGlu₃ G_{α15} calcium assay. In both assays, **44** displays PAM activity. BINA displays PAM activity in the mGlu₂ calcium assay but is inactive in the mGlu₃ calcium assay. For this assay, mGlu₃ expression was induced with 20 ng/mL Tet for 20 h prior to assay. Data were analyzed using nonlinear regression, providing EC₅₀ values for each curve. Data were obtained from three separate experiments performed in triplicate, normalized to the response to 100 μ M glutamate in each experiment, and are expressed as the mean \pm SEM.

Table 6. In Vivo PK for mGlu_{2/3} PAMs in Rats after ip Administration (10 mg/kg)^a

compd	plasma (μ M) ^a	plasma $t_{1/2}$ (min)	brain (μ M) ^a	brain/plasma
44	10.57 \pm 2.52	43	0.23 \pm 0.10	0.03 \pm 0.01
50	3.29 \pm 1.27	20	ND	ND
60	4.49 \pm 0.49	22	ND	ND
65	5.44 \pm 2.92	30	ND	ND
68	2.18 \pm 0.58	28	ND	ND
72	2.44 \pm 2.19	27	ND	ND
73	6.81 \pm 0.84	132	0.47 \pm 0.35	0.02 \pm 0.01
74	17.05 \pm 0.19	106	0.56 \pm 0.10	0.03 \pm 0.01
75	6.52 \pm 0.54	80	0.22 \pm 0.04	0.01 \pm 0.01

^aMaximum concentration of the compound detected in plasma or brain. $t_{1/2}$: terminal half-life. Compounds were dosed ip ($n = 3$) at 10 mg/kg in 10% EtOH/1% Tween 80. pH was adjusted to \sim 7. Brains and plasma were harvested at the T_{max} (30 min for all tested). ND = not determined.

and food-maintained responding.^{37,53} Moreover, the selective mGlu₂ receptor PAM BINA decreased only cocaine-maintained responding while having no effect on food-maintained responding.³⁷ Consistent with our previous results, Morishima et al. (2005) have demonstrated that mGlu₂ receptor knockout mice exhibited increased conditioned place preference for cocaine.⁵⁴ While these prior studies focused only on the role

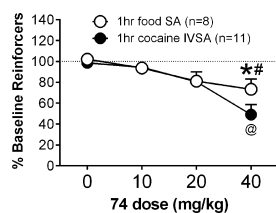


Figure 8. The mGlu_{2/3} PAM, 74, decreased cocaine-maintained responding, and to a lesser extent food-maintained responding, in rats. At the highest dose tested (40 mg/kg), cocaine-maintained responding was significantly lower than food-maintained responding. The 40 mg/kg dose decreased responding for food compared to vehicle only, whereas the same dose decreased responding for cocaine compared to all other doses tested. (*) Responding was significantly different from 0 mg/kg. (#) Responding was significantly different from cocaine. (@) Responding was significantly different from 0, 10, and 20 mg/kg. Data are expressed as the mean \pm SEM of responding at baseline.

of mGlu₂ receptors in responding for drug and natural rewards, our present findings begin to delineate the individual roles of mGlu₂ and mGlu₃ receptors in reward processing. These patterns of results possibly suggest that activation of mGlu₂ receptors selectively modulates drug-reinforced behavior, whereas activation of mGlu₃ receptors either selectively modulates responding for natural rewards or nonselectively modulates responding for both drug and natural rewards. Use of an mGlu_{2/3} receptor PAM, as reported here, provided an initial tool by which to indirectly test these hypotheses. However, future development and use of selective mGlu₃ receptor PAMs are necessary to test these hypotheses directly. Moreover, increasing mGlu_{2/3} receptor activity using a PAM compared to a receptor agonist may affect behaviors reinforced by natural rewards to a lesser extent relative to drug-reinforced behaviors. Thus, targeting mGlu₂ receptors with a PAM may be an effective strategy for treating drug dependence without affecting other motivated behaviors.

In conclusion, a ligand-based rational design approach utilizing certain previously reported selective mGlu₂ receptor PAMs as starting points led to a series of new mGlu_{2/3} PAMs. A library of more than 60 analogues was synthesized and tested, providing compounds with excellent potency and efficacy at mGlu₂ and mGlu₃ receptors in vitro. The most promising mGlu_{2/3} PAMs were profiled in in vitro ADME assays, and on the basis of these data, several compounds were selected for PK studies in rats. The lead structures were found to be essentially devoid of activity at other mGlu receptor subtypes and 45 additional CNS receptors. Representative PAM 44 was characterized extensively in vitro and was found to demonstrate ago-PAM activity at mGlu₂ and PAM activity at mGlu₃ receptors. Finally, the systemically active mGlu_{2/3} PAM 74 dose-dependently decreased cocaine self-administration in rats following a single intraperitoneal dose. Future studies will focus on additional characterization of the new mGlu_{2/3} PAMs and further optimization of compounds with enhanced PAM activity at mGlu₃ receptors.

EXPERIMENTAL SECTION

General Chemistry. All reactions were performed in oven-dried glassware under an atmosphere of argon with magnetic stirring. All solvents and chemicals used were purchased from Sigma-Aldrich or Acros, and were used as received without further purification. Purity of compounds was established by liquid chromatography–mass spectroscopy (HPLC–MS) and was >95% for all tested compounds. Silica gel column chromatography was carried out using prepacked silica cartridges from RediSep (ISCO Ltd.) and eluted using an Isco

Companion system. ¹H and ¹³C NMR spectra were obtained on a Jeol 400 spectrometer at 400 and 100 MHz, respectively. Chemical shifts are reported in δ (ppm) relative to residual solvent peaks or TMS as internal standards. Coupling constants are reported in Hz. Melting points were obtained using a capillary melting point apparatus (MEL-TEMP) and are uncorrected. High-resolution ESI-TOF mass spectra were acquired from the Mass Spectrometry Core at The Sanford-Burnham Medical Research Institute (Orlando, FL). HPLC–MS analyses were performed on a Shimadzu 2010EV LCMS instrument using the following conditions: Kromasil C18 column (reverse phase, 4.6 mm \times 50 mm); a linear gradient from 10% acetonitrile and 90% water to 95% acetonitrile and 5% water over 4.5 min; flow rate of 1 mL/min; UV photodiode array detection from 200 to 300 nm.

General Methods for the Synthesis of mGlu_{2/3} Receptor PAMs. *General Method A.* To a stirred solution of methyl 4-hydroxybenzoate (1 mmol, 1 equiv) and 1,4-dibromobutane (3 mmol, 3 equiv) in ACN was added potassium carbonate (2 mmol, 2 equiv). The reaction mixture was heated at reflux for 6 h, at which time it was cooled to room temperature. The crude reaction mixture was diluted with CH₂Cl₂ and washed twice with 5% aqueous HCl (200 mL). The organic layers were collected and washed twice with saturated NaHCO₃ solution (200 mL). The organic layers were collected, dried over Na₂SO₄, and evaporated to dryness. To a stirred solution of AlCl₃ (0.039 mol, 1 equiv) in CH₂Cl₂ at 0 °C under nitrogen, the acyl chloride (0.039 mol, 1 equiv) was dissolved in CH₂Cl₂ and added dropwise to the stirred solution. The phenol (0.039 mol, 1 equiv) was added to the reaction mixture, and the mixture was allowed to warm to room temperature over 12 h. The reaction was quenched with HCl (5% aqueous), and CH₂Cl₂ was added (50 mL). The organic layer was separated and washed with saturated NaHCO₃ solution, then brine and dried over Na₂SO₄. The solvents were removed by rotary evaporation, and the products were isolated by flash chromatography [SiO₂, hexanes/EtOAc (4:1)] and concentrated in vacuo. To a crimp top microwave vial were added the phenol (1 mmol, 1 equiv), bromobutoxy benzoate (1 mmol, 1 equiv), potassium carbonate (2 mmol, 2 equiv), and potassium iodide (0.1 mmol, 0.1 equiv), all dissolved in ACN (0.2 M). The reaction mixture was heated in the microwave at 160 °C for 15 min. Following filtration and evaporation of solvents, the products were isolated by flash chromatography or reverse phase HPLC and lyophilized to provide the final compounds which were determined to be >95% pure by HPLC–UV, HPLC–MS, and ¹H NMR.

General Method B. To a stirred solution of the product from “General Method A” (1 mmol, 1 equiv) in dioxane at room temperature was added KOH (6 mmol, 6 equiv) in water (0.5 mL). The mixture was stirred continuously for an additional 12 h. The reaction was quenched with HCl (5% aqueous), and CH₂Cl₂ (50 mL) was added. The organic layer was separated and dried over Na₂SO₄. The solvents were removed by rotary evaporation, and the products were isolated by flash chromatography [SiO₂, hexanes/EtOAc (1:1)] or reverse phase HPLC and lyophilized to provide the final compounds which were determined to be >95% pure by HPLC–UV, HPLC–MS, and ¹H NMR. Compounds 4, 5, and 6 were synthesized according to the published procedures.^{50,51} The following compounds were prepared using the general procedures A and B from the appropriate starting materials.

Methyl 4-(4-(2,3-Dimethyl-4-(3-methylbutanoyl)phenoxy)butoxy)benzoate (14). 14 was prepared according to general procedure A. Colorless solid (0.070 g, 17%); mp 55–57 °C. ¹H NMR (CDCl₃): δ 7.86 (d, J = 7.8 Hz, 2H), 7.17–6.94 (m, 4H), 4.05 (t, J = 5.9 Hz, 2H), 3.88 (s, 3H), 3.80 (t, J = 6.0 Hz, 2H), 2.81 (d, J = 6.9 Hz, 2H), 2.29 (s, 3H), 2.20 (s, 3H), 2.10–2.01 (m, 1H), 1.88–1.84 (m, 4H), 0.93 (d, J = 6.4 Hz, 6H). ¹³C NMR (CDCl₃): δ 203.3, 166.8, 162.7, 155.5, 142.3, 132.2, 131.5, 130.6, 125.7, 125.4, 122.5, 114.0, 75.1, 67.7, 51.8, 51.7, 26.9, 25.9, 25.1, 22.63, 20.0, 12.3. ESI-MS m/z 413 [M + H]⁺. HRMS m/z calcd for C₂₅H₃₂O₅ [M + H]⁺: 413.2323. Found: 413.2256.

Methyl 4-(4-(2-Cyclopentylacetyl)-2,3-dimethylphenoxy)butoxy)benzoate (15). 15 was prepared according to general procedure A. Colorless solid (0.039 g, 9%). ¹H NMR (CDCl₃): δ 7.87 (d, J = 9.2 Hz, 2H), 7.17 (d, J = 7.8 Hz, 1H), 7.00–6.97 (m, 3H), 4.05 (t, J = 5.9 Hz, 2H), 3.88 (s, 3H), 3.80 (t, J = 5.9 Hz, 2H), 2.95 (d, J = 6.9 Hz, 2H), 2.29 (s, 3H), 2.20 (s, 3H), 2.21–2.10 (m, 1H), 1.99–1.89

(m, 4H), 1.80–1.76 (m, 2H), 1.59–1.46 (m, 4H), 1.14–1.01 (m, 2H). ^{13}C NMR (CDCl_3): δ 203.3, 166.8, 162.7, 155.5, 142.3, 132.2, 131.5, 130.6, 126.9, 126.2, 114.0, 74.7, 67.7, 51.8, 49.0, 36.1, 32.7, 26.9, 25.9, 24.9, 20.0, 12.3. ESI-MS m/z 439 $[\text{M} + \text{H}]^+$. HRMS m/z calcd for $\text{C}_{27}\text{H}_{34}\text{O}_5$ $[\text{M} + \text{H}]^+$: 439.2479. Found: 439.2419.

Methyl 4-(4-(3-Hydroxy-2-methyl-4-(3-methylbutanoyl)phenoxy)butoxy)benzoate (16). 16 was prepared according to general procedure A. Colorless solid (0.112 g, 27%); mp 72–74 °C. ^1H NMR (CDCl_3): δ 7.98–7.96 (m, 2H), 7.58 (d, J = 8.7 Hz, 1H), 6.90–6.88 (m, 2H), 6.41 (d, J = 9.2 Hz, 1H), 4.09–4.03 (m, 4H), 3.86 (s, 3H), 2.76 (d, J = 7.3 Hz, 2H), 2.20–2.15 (m, 1H), 2.09 (s, 3H), 1.96–1.94 (m, 4H), 0.97 (d, J = 6.9 Hz, 6H). ^{13}C NMR (CDCl_3): δ 205.1, 166.8, 162.6, 162.5, 162.3, 131.5, 129.3, 122.5, 114.0, 113.7, 102.8, 76.7, 67.5, 51.8, 46.8, 26.9, 26.8, 25.9, 22.7, 7.6. ESI-MS m/z 415 $[\text{M} + \text{H}]^+$. HRMS m/z calcd for $\text{C}_{24}\text{H}_{30}\text{O}_6$ $[\text{M} + \text{H}]^+$: 415.2115. Found: 415.2137.

Methyl 4-(4-(4-(2-Cyclopentylacetyl)-3-hydroxy-2-methylphenoxy)butoxy)benzoate (17). 17 was prepared according to general procedure A. Colorless solid (0.277 g, 63%). ^1H NMR (CDCl_3): δ 7.86 (d, J = 8.7 Hz, 2H), 7.79 (d, J = 8.7 Hz, 1H), 6.90 (d, J = 9.2 Hz, 2H), 6.61 (d, J = 9.2 Hz, 1H), 4.11–4.09 (m, 4H), 3.87 (s, 3H), 2.90 (d, J = 7.3 Hz, 2H), 2.35–2.20 (m, 1H), 1.96 (s, 3H), 1.94–1.92 (m, 4H), 1.85–1.76 (m, 2H), 1.59–1.47 (m, 4H), 1.87–1.19 (m, 2H). ^{13}C NMR (CDCl_3): δ 205.3, 162.6, 162.5, 162.3, 131.6, 129.2, 122.5, 114.0, 113.8, 113.7, 102.4, 67.7, 67.5, 51.8, 44.0, 36.8, 32.6, 25.9, 24.8, 7.6. ESI-MS m/z 441 $[\text{M} + \text{H}]^+$. HRMS m/z calcd for $\text{C}_{26}\text{H}_{32}\text{O}_6$ $[\text{M} + \text{H}]^+$: 441.2272. Found: 441.2278.

4-(4-(2,3-Dimethyl-4-(3-methylbutanoyl)phenoxy)butoxy)benzoic Acid (18). Colorless solid (0.159 g, 40%). ^1H NMR (DMSO): δ 7.84 (d, J = 8.7 Hz, 2H), 7.20 (d, J = 8.2 Hz, 1H), 6.99 (d, J = 8.7 Hz, 3H), 4.11 (t, J = 5.5 Hz, 2H), 3.75 (t, J = 5.5 Hz, 2H), 2.78 (d, J = 6.9 Hz, 2H), 2.24 (s, 3H), 2.15 (s, 3H), 2.02–1.98 (m, 1H), 1.87–1.80 (m, 4H), 0.86 (d, J = 6.9 Hz, 6H). ^{13}C NMR (DMSO): δ 203.6, 167.0, 162.1, 155.1, 142.1, 131.7, 131.3, 130.4, 125.9, 125.2, 123.1, 114.2, 74.5, 67.5, 51.1, 27.2, 26.3, 25.3, 24.5, 22.3, 20.0, 12.0. ESI-MS m/z 399 $[\text{M} + \text{H}]^+$. HRMS m/z calcd for $\text{C}_{24}\text{H}_{30}\text{O}_5$ $[\text{M} + \text{H}]^+$: 399.2166. Found: 399.2191.

4-(4-(4-(2-Cyclopentylacetyl)-2,3-dimethylphenoxy)butoxy)benzoic Acid (19). Colorless solid (0.093 g, 22%). ^1H NMR (DMSO): δ 7.83 (d, J = 8.7 Hz, 2H), 7.21 (d, J = 7.8 Hz, 1H), 6.98 (d, J = 8.7 Hz, 3H), 4.12 (t, J = 5.5 Hz, 2H), 3.75 (t, J = 5.5 Hz, 2H), 2.90 (d, J = 6.9 Hz, 2H), 2.25 (s, 3H), 2.14 (s, 3H), 2.09–2.07 (m, 1H), 1.86–1.84 (m, 4H), 1.69–1.62 (m, 2H), 1.51–1.37 (m, 4H), 1.04–0.98 (m, 2H). ^{13}C NMR (DMSO): δ 207.8, 167.0, 162.3, 154.2, 142.1, 131.4, 130.4, 125.8, 125.6, 122.9, 114.3, 74.1, 67.9, 49.3, 35.6, 32.1, 25.6, 25.1, 24.5, 20.2, 12.1. ESI-MS m/z 425 $[\text{M} + \text{H}]^+$. HRMS m/z calcd for $\text{C}_{26}\text{H}_{32}\text{O}_5$ $[\text{M} + \text{H}]^+$: 425.2323. Found: 425.2366.

4-(4-(3-Hydroxy-2-methyl-4-(3-methylbutanoyl)phenoxy)butoxy)benzoic Acid (20). Colorless solid (0.208 g, 52%); mp 153–155 °C. ^1H NMR (DMSO): δ 7.84 (d, J = 8.7 Hz, 2H), 7.76 (d, J = 8.7 Hz, 1H), 6.96 (d, J = 9.2 Hz, 2H), 6.60 (d, J = 9.2 Hz, 1H), 4.11–4.06 (m, 4H), 2.79 (d, J = 6.9 Hz, 2H), 2.10–2.08 (m, 1H), 1.93 (s, 3H), 1.89–1.86 (m, 4H), 0.89 (d, J = 6.9 Hz, 6H). ^{13}C NMR (DMSO): δ 206.2, 167.0, 162.5, 162.3, 161.4, 131.4, 130.4, 122.9, 114.3, 113.5, 112.0, 103.4, 67.7, 67.5, 51.8, 44.0, 36.8, 32.6, 25.4, 22.4, 7.6. ESI-MS m/z 401 $[\text{M} + \text{H}]^+$. HRMS m/z calcd for $\text{C}_{23}\text{H}_{28}\text{O}_6$ $[\text{M} + \text{H}]^+$: 401.1956. Found: 401.1966.

4-(4-(4-(2-Cyclopentylacetyl)-3-hydroxy-2-methylphenoxy)butoxy)benzoic Acid (21). Colorless solid (0.192 g, 45%); mp 158–160 °C. ^1H NMR (DMSO): δ 7.83–7.81 (m, 3H), 6.69 (d, J = 8.7 Hz, 2H), 6.59 (d, J = 8.7 Hz, 1H), 4.11–4.08 (m, 4H), 2.97 (d, J = 6.9 Hz, 2H), 2.22–2.01 (m, 1H), 1.96 (s, 3H), 1.89–1.86 (m, 4H), 1.72–1.71 (m, 2H), 1.59–1.55 (m, 2H), 1.45–1.53 (m, 2H), 1.15–1.12 (m, 2H). ^{13}C NMR (DMSO): δ 207.8, 167.0, 162.5, 162.3, 161.4, 131.6, 131.3, 122.9, 114.2, 112.8, 111.9, 103.8, 69.0, 68.9, 43.8, 36.2, 31.1, 24.5, 22.4, 8.9. ESI-MS m/z 427 $[\text{M} + \text{H}]^+$. HRMS m/z calcd for $\text{C}_{25}\text{H}_{30}\text{O}_6$ $[\text{M} + \text{H}]^+$: 427.2115. Found: 427.2120.

3-(4-(2,3-Dimethyl-4-(3-methylbutanoyl)phenoxy)butoxy)benzoic Acid (22). Colorless solid (0.167 g, 42%). ^1H NMR (DMSO): δ 7.49–7.46 (m, 2H), 7.41–7.39 (m, 2H), 7.16–7.14 (m,

1H), 6.73–6.69 (m, 1H), 4.04–4.03 (m, 4H), 2.74 (d, J = 6.9 Hz, 2H), 2.11 (s, 3H), 2.03 (s, 3H), 1.90–1.87 (m, 1H), 1.86–1.84 (m, 4H), 0.82 (d, J = 6.9 Hz, 6H). ^{13}C NMR (DMSO): δ 205.6, 167.2, 162.9, 161.4, 158.6, 132.7, 131.4, 129.7, 124.7, 121.8, 119.8, 114.2, 109.8, 74.2, 67.6, 51.7, 25.6, 25.3, 22.4, 24.1, 19.9, 19.8, 12.0, 11.9. ESI-MS m/z 399 $[\text{M} + \text{H}]^+$. HRMS m/z calcd for $\text{C}_{24}\text{H}_{30}\text{O}_5$ $[\text{M} + \text{H}]^+$: 399.2166. Found: 399.2239.

3-(4-(4-(2-Cyclopentylacetyl)-2,3-dimethylphenoxy)butoxy)benzoic Acid (23). Colorless solid (0.114 g, 27%). ^1H NMR (DMSO): δ 7.47–7.40 (m, 3H), 7.19–7.15 (m, 2H), 6.97 (d, J = 7.8 Hz, 1H), 4.04 (t, J = 5.6 Hz, 2H), 3.73 (t, J = 5.9 Hz, 2H), 2.89 (d, J = 6.9 Hz, 2H), 2.21 (s, 3H), 2.11–2.04 (overlapping singlet and multiplets, 4H), 1.85–1.83 (m, 4H), 1.66–1.64 (m, 2H), 1.48–1.39 (m, 4H), 1.04–1.01 (m, 2H). ^{13}C NMR (DMSO): δ 205.6, 167.2, 167.2, 158.2, 155.2, 141.9, 132.7, 131.4, 130.2, 129.7, 125.9, 125.2, 121.8, 119.3, 114.5, 74.4, 67.6, 48.4, 35.5, 32.0, 26.3, 25.4, 24.5, 20.0, 11.9. ESI-MS m/z 425 $[\text{M} + \text{H}]^+$. HRMS m/z calcd for $\text{C}_{26}\text{H}_{32}\text{O}_5$ $[\text{M} + \text{H}]^+$: 425.2323. Found: 425.2383.

3-(4-(3-Hydroxy-2-methyl-4-(3-methylbutanoyl)phenoxy)butoxy)benzoic Acid (24). Colorless solid (0.148 g, 37%); mp 118–120 °C. ^1H NMR (DMSO): δ 7.81 (d, J = 9.2 Hz, 1H), 7.46 (d, J = 7.8 Hz, 1H), 7.39–7.34 (m, 2H), 7.14–7.13 (m, 1H), 6.58 (d, J = 9.2 Hz, 1H), 4.13 (t, J = 5.9 Hz, 2H), 4.07 (t, J = 5.9 Hz, 2H), 2.81 (d, J = 6.9 Hz, 2H), 2.11–2.08 (m, 1H), 1.95 (s, 3H), 1.88–1.86 (m, 4H), 0.91 (d, J = 6.9 Hz, 6H). ^{13}C NMR (DMSO): δ 205.6, 167.2, 162.5, 161.4, 158.6, 132.3, 130.4, 129.7, 121.6, 119.4, 114.5, 113.5, 112.0, 103.4, 67.9, 67.3, 46.0, 25.6, 25.4, 22.5, 7.5. ESI-MS m/z 401 $[\text{M} + \text{H}]^+$. HRMS m/z calcd for $\text{C}_{23}\text{H}_{28}\text{O}_6$ $[\text{M} + \text{H}]^+$: 401.1959. Found: 401.1967.

3-(4-(4-(2-Cyclopentylacetyl)-3-hydroxy-2-methylphenoxy)butoxy)benzoic Acid (25). Colorless solid (0.230 g, 54%); mp 125–127 °C. ^1H NMR (DMSO): δ 7.76 (d, J = 9.2 Hz, 1H), 7.46 (d, J = 7.8 Hz, 1H), 7.41–7.33 (m, 2H), 7.13–7.12 (m, 1H), 6.58 (d, J = 9.2 Hz, 1H), 4.08–4.03 (m, 4H), 2.94 (d, J = 7.3 Hz, 2H), 2.17–2.16 (m, 1H), 1.95 (s, 3H), 1.87–1.85 (m, 4H), 1.71–1.68 (m, 2H), 1.55–1.42 (m, 4H), 1.12–1.09 (m, 2H). ^{13}C NMR (DMSO): δ 205.8, 162.5, 161.3, 158.6, 132.3, 130.3, 129.7, 121.6, 119.4, 114.6, 113.3, 112.0, 103.3, 67.9, 67.4, 43.6, 36.3, 32.1, 25.4, 24.5, 7.5. ESI-MS m/z 427 $[\text{M} + \text{H}]^+$. HRMS m/z calcd for $\text{C}_{25}\text{H}_{30}\text{O}_6$ $[\text{M} + \text{H}]^+$: 427.2115. Found: 427.2122.

2-(4-(2,3-Dimethyl-4-(3-methylbutanoyl)phenoxy)butoxy)benzoic Acid (26). Colorless solid (0.207 g, 52%); mp 48–50 °C. ^1H NMR (DMSO): δ 7.58 (d, J = 7.8 Hz, 1H), 7.45 (t, J = 7.8 Hz, 1H), 7.11–6.99 (m, 3H), 6.73–6.68 (m, 1H), 4.09–4.04 (m, 4H), 2.77 (d, J = 7.3 Hz, 2H), 2.24 (s, 3H), 2.18 (s, 3H), 2.01–2.00 (m, 1H), 1.89–1.86 (m, 4H), 0.86 (d, J = 6.8 Hz, 6H). ^{13}C NMR (DMSO): δ 205.8, 167.4, 157.5, 156.5, 137.2, 133.0, 130.7, 125.9, 121.9, 120.1, 113.5, 109.3, 67.9, 67.4, 51.2, 48.7, 25.6, 24.6, 22.4, 19.8, 12.1, 11.5. ESI-MS m/z 399 $[\text{M} + \text{H}]^+$. HRMS m/z calcd for $\text{C}_{24}\text{H}_{30}\text{O}_5$ $[\text{M} + \text{H}]^+$: 399.2166. Found: 399.2284.

2-(4-(4-(2-Cyclopentylacetyl)-2,3-dimethylphenoxy)butoxy)benzoic Acid (27). Colorless solid (0.199 g, 47%); mp 90–92 °C. ^1H NMR (DMSO): δ 7.59 (d, J = 7.9 Hz, 1H), 7.46–7.44 (m, 2H), 7.06 (d, J = 8.2 Hz, 1H), 6.92 (t, J = 7.8 Hz, 1H), 6.81 (d, J = 8.7 Hz, 1H), 4.05–4.04 (m, 4H), 2.79 (d, J = 6.9 Hz, 2H), 2.24 (s, 3H), 2.19 (s, 3H), 2.11–2.04 (m, 1H), 1.89–1.86 (m, 4H), 1.66–1.64 (m, 2H), 1.51–1.40 (m, 4H), 1.05–1.02 (m, 2H). ^{13}C NMR (DMSO): δ 204.1, 167.5, 158.1, 157.4, 136.7, 132.8, 132.2, 130.6, 127.4, 125.5, 121.7, 120.0, 113.4, 107.9, 67.8, 67.5, 47.6, 36.1, 32.0, 25.5, 24.5, 16.5, 11.5. ESI-MS m/z 425 $[\text{M} + \text{H}]^+$. HRMS m/z calcd for $\text{C}_{26}\text{H}_{32}\text{O}_5$ $[\text{M} + \text{H}]^+$: 425.2323. Found: 425.2357.

2-(4-(3-Hydroxy-2-methyl-4-(3-methylbutanoyl)phenoxy)butoxy)benzoic Acid (28). Colorless solid (0.164 g, 41%); mp 101–103 °C. ^1H NMR (DMSO): δ 7.78 (d, J = 8.7 Hz, 1H), 7.59 (d, J = 9.6 Hz, 1H), 7.42–7.41 (m, 1H), 7.06 (d, J = 8.3 Hz, 1H), 6.95 (t, J = 7.4 Hz, 1H), 6.60 (d, J = 9.2 Hz, 1H), 4.11–4.07 (m, 4H), 2.79 (d, J = 6.9 Hz, 2H), 2.09–2.02 (m, 1H), 1.95 (s, 3H), 1.89–1.86 (m, 4H), 0.90 (d, J = 6.4 Hz, 6H). ^{13}C NMR (CDCl_3): δ 205.6, 167.4, 162.5, 161.3, 157.4, 132.9, 130.6, 130.3, 121.6, 120.0, 113.4, 111.9, 103.3, 67.9, 67.8, 45.8, 36.3, 25.4, 22.4, 7.5. ESI-MS m/z 401 $[\text{M} + \text{H}]^+$.

HRMS m/z calcd for $C_{23}H_{28}O_6$ $[M + H]^+$: 401.1959. Found: 401.1990.

2-(4-(4-(2-Cyclopentylacetyl)-3-hydroxy-2-methylphenoxy)butoxy)benzoic Acid (29). Colorless solid (0.158 g, 37%); mp 93–95 °C. 1H NMR (DMSO): δ 7.78 (d, J = 8.7 Hz, 1H), 7.62 (d, J = 9.6 Hz, 1H), 7.45 (t, J = 7.6 Hz, 1H), 7.10 (d, J = 8.2 Hz, 1H), 6.69 (t, J = 7.3 Hz, 1H), 6.63 (d, J = 9.2 Hz, 1H), 4.14–4.11 (m, 4H), 2.98 (d, J = 6.8 Hz, 2H), 2.23–2.18 (m, 1H), 1.97 (s, 3H), 1.92–1.87 (m, 4H), 1.75–1.71 (m, 2H), 1.58–1.47 (m, 4H), 1.15–1.11 (m, 2H). ^{13}C NMR (DMSO): δ 205.8, 167.4, 162.5, 161.3, 157.4, 132.9, 130.6, 130.3, 121.6, 120.0, 113.4, 113.2, 103.3, 111.9, 67.8, 67.9, 43.9, 36.3, 32.0, 25.6, 24.4, 7.5. ESI-MS m/z 427 $[M + H]^+$. HRMS m/z calcd for $C_{25}H_{30}O_6$ $[M + H]^+$: 427.2115. Found: 427.2235.

2-Chloro-4-(4-(2,3-dimethyl-4-(3-methylbutanoyl)phenoxy)butoxy)benzoic Acid (30). Colorless solid (0.078 g, 18%); mp 77–79 °C. 1H NMR (DMSO): δ 7.72–7.68 (m, 1H), 7.09 (d, J = 7.8 Hz, 1H), 6.91–4–6.91 (m, 3H), 4.06–4.03 (m, 4H), 2.62 (d, J = 6.9 Hz, 2H), 2.11 (s, 3H), 2.01 (s, 3H), 1.88–1.86 (m, 4H), 1.74–1.72 (m, 1H), 0.78 (d, J = 6.4 Hz, 6H). ^{13}C NMR (DMSO): δ 204.1, 167.5, 162.0, 155.6, 143.3, 134.1, 133.9, 131.8, 131.7, 126.0, 125.9, 122.3, 117.1, 113.8, 75.8, 69.9, 51.7, 26.1, 25.8, 25.2, 22.8, 20.6, 12.5. ESI-MS m/z 433 $[M + H]^+$. HRMS m/z calcd for $C_{24}H_{29}ClO_5$ $[M + H]^+$: 433.1776. Found: 433.1799.

2-Chloro-4-(4-(4-(2-cyclopentylacetyl)-2,3-dimethylphenoxy)butoxy)benzoic Acid (31). Colorless solid (0.115 g, 25%); mp 97–99 °C. 1H NMR (DMSO): δ 7.68 (d, J = 8.2 Hz, 1H), 7.38 (d, J = 8.7 Hz, 1H), 6.88 (s, 1H), 6.88 (d, J = 8.7 Hz, 1H), 6.74 (d, J = 8.7 Hz, 1H), 4.07–4.03 (m, 4H), 2.71 (d, J = 6.9 Hz, 2H), 2.10 (s, 3H), 1.98–1.94 (m, 1H), 1.95 (s, 3H), 1.79–1.77 (m, 4H), 1.66–1.64 (m, 2H), 1.51–1.40 (m, 4H), 1.05–1.02 (m, 2H). ^{13}C NMR (DMSO): δ 205.8, 166.0, 162.5, 161.4, 133.2, 130.4, 122.3, 116.6, 113.5, 111.7, 103.4, 68.0, 67.8, 46.0, 26.1, 25.6, 25.3, 25.1, 22.5, 7.5. ESI-MS m/z 459 $[M + H]^+$. HRMS m/z calcd for $C_{26}H_{31}ClO_5$ $[M + H]^+$: 459.1933. Found: 459.1942.

2-Chloro-4-(4-(4-(2-cyclopentylacetyl)-3-hydroxy-2-methylphenoxy)butoxy)benzoic Acid (32). Colorless solid (0.191 g, 44%); mp 113–115 °C. 1H NMR (DMSO): δ 7.78 (d, J = 8.7 Hz, 2H), 7.00 (s, 1H), 6.94 (d, J = 8.7 Hz, 1H), 6.60 (d, J = 9.2 Hz, 1H), 4.10–4.08 (m, 4H), 2.80 (d, J = 6.9 Hz, 2H), 2.13–2.01 (m, 1H), 1.92 (s, 3H), 1.89–1.86 (m, 4H), 0.90 (d, J = 6.4 Hz, 6H). ^{13}C NMR (DMSO): δ 205.8, 166.0, 162.5, 161.4, 133.2, 130.4, 122.3, 116.6, 113.5, 111.7, 103.4, 68.0, 67.8, 46.0, 26.1, 25.6, 25.3, 25.1, 22.5, 7.5. ESI-MS m/z 435 $[M + H]^+$. HRMS m/z calcd for $C_{23}H_{27}ClO_6$ $[M + H]^+$: 435.1569. Found: 435.1563.

2-Chloro-4-(4-(4-(2-cyclopentylacetyl)-3-hydroxy-2-methylphenoxy)butoxy)benzoic Acid (33). Colorless solid (0.168 g, 30%); mp 130–132 °C. 1H NMR (DMSO): δ 7.78 (d, J = 8.7 Hz, 2H), 7.03 (s, 1H), 7.00 (d, J = 9.2 Hz, 1H), 6.58 (d, J = 9.2 Hz, 1H), 4.10–4.08 (m, 4H), 2.95 (d, J = 7.3 Hz, 2H), 2.21–2.19 (m, 1H), 1.94 (s, 3H), 1.89–1.86 (m, 4H), 1.77–1.71 (m, 2H), 1.56–1.45 (m, 4H), 1.13–1.10 (m, 2H). ^{13}C NMR (DMSO): δ 205.8, 166.0, 162.5, 161.4, 133.2, 130.4, 122.3, 116.6, 113.5, 111.7, 103.4, 68.0, 67.8, 46.0, 26.1, 25.6, 25.3, 25.1, 22.5, 7.5. ESI-MS m/z 461 $[M + H]^+$. HRMS m/z calcd for $C_{25}H_{29}ClO_6$ $[M + H]^+$: 461.1725. Found: 461.1721.

5-(4-(2,3-Dimethyl-4-(3-methylbutanoyl)phenoxy)butoxy)-2-fluorobenzoic Acid (34). Colorless solid (0.133 g, 32%). 1H NMR (DMSO): δ 7.27–7.15 (m, 4H), 6.94 (d, J = 7.8 Hz, 1H), 3.98–3.68 (m, 4H), 2.71 (d, J = 6.9 Hz, 2H), 2.19 (s, 3H), 2.09 (s, 3H), 2.05–1.95 (m, 1H), 1.89–1.81 (m, 4H), 0.80 (d, J = 6.4 Hz, 6H). ^{13}C NMR (DMSO): δ 202.9, 155.2, 154.4, 142.2, 131.8, 130.5, 126.0, 125.3, 120.6, 118.0, 117.7, 116.1, 74.5, 68.1, 51.1, 26.3, 25.5, 24.6, 22.4, 20.1, 12.0. ESI-MS m/z 417 $[M + H]^+$. HRMS m/z calcd for $C_{25}H_{29}FO_5$ $[M + H]^+$: 417.2072. Found: 417.2116.

5-(4-(4-(2-Cyclopentylacetyl)-2,3-dimethylphenoxy)butoxy)-2-fluorobenzoic Acid (35). Colorless solid (0.177 g, 40%); mp 118–120 °C. 1H NMR (DMSO): δ 7.44 (d, J = 8.2 Hz, 1H), 7.27–7.11 (m, 3H), 6.77 (d, J = 8.7 Hz, 1H), 3.98–3.70 (m, 4H), 2.77 (d, J = 7.3 Hz, 2H), 2.18 (s, 3H), 2.10–2.01 (m, 1H), 2.02 (s, 3H), 1.89–1.83 (m, 4H), 1.67–1.64 (m, 2H), 1.48–1.38 (m, 4H), 1.05–1.03 (m, 2H). ^{13}C NMR (DMSO): δ 204.0, 165.0, 158.1, 154.3, 136.8, 132.2,

127.3, 125.6, 117.8, 117.6, 116.0, 107.9, 67.9, 67.4, 47.6, 36.1, 32.0, 25.6, 24.5, 16.5, 11.4. ESI-MS m/z 443 $[M + H]^+$. HRMS m/z calcd for $C_{26}H_{31}FO_5$ $[M + H]^+$: 443.2228. Found: 443.2214.

2-Fluoro-5-(4-(3-hydroxy-2-methyl-4-(3-methylbutanoyl)phenoxy)butoxy)benzoic Acid (36). Colorless solid (0.188 g, 45%); mp 99–101 °C. 1H NMR (DMSO): δ 7.76 (d, J = 9.2 Hz, 1H), 7.28–7.15 (m, 3H), 6.58 (d, J = 9.2 Hz, 1H), 4.10–4.03 (m, 4H), 2.78 (d, J = 7.3 Hz, 2H), 2.10–2.01 (m, 1H), 1.94 (s, 3H), 1.87–1.84 (m, 4H), 0.89 (d, J = 6.9 Hz, 6H). ^{13}C NMR (DMSO): δ 205.7, 165.0, 162.5, 161.4, 154.4, 130.4, 121.3, 117.8, 116.0, 113.5, 112.0, 103.4, 67.9, 67.8, 46.0, 25.6, 25.5, 22.5, 7.5. ESI-MS m/z 419 $[M + H]^+$. HRMS m/z calcd for $C_{23}H_{27}FO_6$ $[M + H]^+$: 419.1864. Found: 419.1863.

5-(4-(4-(2-Cyclopentylacetyl)-3-hydroxy-2-methylphenoxy)butoxy)-2-fluorobenzoic Acid (37). Colorless solid (0.208 g, 47%); mp 110–112 °C. 1H NMR (DMSO): δ 7.76 (d, J = 9.2 Hz, 1H), 7.28 (d, J = 8.7 Hz, 1H), 7.15–7.13 (m, 2H), 6.59 (d, J = 9.2 Hz, 1H), 4.10–4.03 (m, 4H), 2.94 (d, J = 7.3 Hz, 2H), 2.20–2.10 (m, 1H), 1.94 (s, 3H), 1.87–1.84 (m, 4H), 1.72–1.70 (m, 2H), 1.56–1.44 (m, 4H), 1.12–1.01 (m, 2H). ^{13}C NMR (DMSO): δ 206.5, 165.0, 162.5, 161.3, 154.4, 130.3, 121.3, 118.0, 117.8, 116.0, 113.3, 112.0, 103.3, 67.9, 67.8, 44.0, 36.0, 32.1, 25.5, 25.4, 24.5, 7.5. ESI-MS m/z 445 $[M + H]^+$. HRMS m/z calcd for $C_{25}H_{29}FO_6$ $[M + H]^+$: 445.2021. Found: 445.2027.

3-[4-(3-Hydroxy-2-methyl-4-(3-methylbutanoyl)phenoxy)butoxy]-4-methylbenzoic Acid (38). Colorless solid (0.277 g, 67%); mp 151–153 °C. 1H NMR (DMSO): δ 7.79 (d, J = 9.2 Hz, 1H), 7.43–7.41 (m, 2H), 7.20 (d, J = 7.8 Hz, 1H), 6.60 (d, J = 8.7 Hz, 1H), 4.14–4.10 (m, 4H), 2.81 (d, J = 6.9 Hz, 2H), 2.15 (s, 3H), 2.13–2.12 (m, 1H), 1.97 (s, 3H), 1.91–1.89 (m, 4H), 0.90 (d, J = 6.9 Hz, 6H). ^{13}C NMR (DMSO): δ 205.8, 167.4, 162.5, 161.3, 157.4, 132.9, 130.6, 130.3, 121.6, 120.0, 113.4, 113.2, 111.9, 103.3, 67.9, 67.8, 43.9, 36.3, 32.0, 25.6, 24.4, 7.5. ESI-MS m/z 415 $[M + H]^+$. HRMS m/z calcd for $C_{24}H_{30}O_6$ $[M + H]^+$: 415.2115. Found: 415.2009.

3-[4-(4-(2-Cyclopentylacetyl)-3-hydroxy-2-methylphenoxy)butoxy]-4-methylbenzoic Acid (39). Colorless solid (0.277 g, 63%). 1H NMR (DMSO): δ 7.79 (d, J = 9.2 Hz, 1H), 7.42–7.40 (m, 2H), 7.20 (d, J = 7.3 Hz, 1H), 6.59 (d, J = 9.2 Hz, 1H), 4.16–4.08 (m, 4H), 2.95 (d, J = 7.3 Hz, 2H), 2.23–2.21 (m, 1H), 2.15 (s, 3H), 1.96 (s, 3H), 1.94–1.90 (m, 4H), 1.73–1.71 (m, 2H), 1.57–1.45 (m, 4H), 1.17–1.14 (m, 2H). ^{13}C NMR (DMSO): δ 205.8, 167.3, 162.4, 161.2, 156.4, 131.3, 130.3, 129.6, 121.4, 113.2, 111.9, 111.2, 103.3, 67.8, 67.2, 43.2, 36.3, 32.0, 25.4, 24.4, 16.1, 7.5. ESI-MS m/z 441 $[M + H]^+$. HRMS m/z calcd for $C_{26}H_{32}O_6$ $[M + H]^+$: 441.2272. Found: 441.2245.

4-[4-(3-Hydroxy-2-methyl-4-(3-methylbutanoyl)phenoxy)butoxy]-3-methylbenzoic Acid (40). Colorless solid (0.282 g, 68%); mp 125–127 °C. 1H NMR (DMSO): δ 7.78 (d, J = 9.2 Hz, 1H), 7.73–7.71 (m, 1H), 7.67 (d, J = 1.4 Hz, 1H), 6.96 (d, J = 8.7 Hz, 1H), 6.59 (d, J = 9.2 Hz, 1H), 4.13–4.10 (m, 4H), 2.80 (d, J = 6.9 Hz, 2H), 2.11 (s, 3H), 2.10–2.07 (m, 1H), 1.93 (s, 3H), 1.92–1.89 (m, 4H), 0.89 (d, J = 6.4 Hz, 6H). ^{13}C NMR (DMSO): δ 205.7, 167.2, 162.4, 161.3, 160.2, 131.5, 130.3, 129.2, 125.7, 122.3, 113.4, 111.9, 110.6, 103.3, 67.8, 67.4, 45.9, 25.4, 22.4, 15.8, 7.5. ESI-MS m/z 415 $[M + H]^+$. HRMS m/z calcd for $C_{24}H_{30}O_6$ $[M + H]^+$: 415.2115. Found: 415.2084.

4-[4-(4-(2-Cyclopentylacetyl)-3-hydroxy-2-methylphenoxy)butoxy]-3-methylbenzoic Acid (41). Colorless solid (0.273 g, 62%). 1H NMR (DMSO): δ 7.78 (d, J = 8.7 Hz, 1H), 7.73 (d, J = 8.7 Hz, 1H), 7.68 (s, 1H), 6.95 (d, J = 8.7 Hz, 1H), 6.58 (d, J = 8.7 Hz, 1H), 4.12–4.08 (m, 4H), 2.94 (d, J = 6.9 Hz, 2H), 2.20–2.01 (m, 1H), 2.12 (s, 3H), 1.93 (s, 3H), 1.90–1.89 (m, 4H), 1.75–1.73 (m, 2H), 1.55–1.44 (m, 4H), 1.13–1.01 (m, 2H). ^{13}C NMR (DMSO): δ 205.8, 167.2, 162.4, 161.2, 160.2, 131.5, 130.3, 129.2, 125.7, 122.3, 113.2, 111.9, 110.6, 103.3, 67.8, 67.4, 43.2, 36.3, 32.0, 25.4, 24.4, 15.8, 7.4. ESI-MS m/z 441 $[M + H]^+$. HRMS m/z calcd for $C_{26}H_{32}O_6$ $[M + H]^+$: 441.2272. Found: 441.2270.

3-Fluoro-4-[4-(3-hydroxy-2-methyl-4-(3-methylbutanoyl)phenoxy)butoxy]benzoic Acid (42). Colorless solid (0.188 g, 45%). 1H NMR (DMSO): δ 7.80 (d, J = 8.7 Hz, 1H), 7.70 (d, J = 9.2 Hz,

1H), 7.61–7.59 (m, 1H), 7.23 (t, $J = 8.5$ Hz, 1H), 6.60 (d, $J = 9.2$ Hz, 1H), 4.18–4.13 (m, 4H), 2.81 (d, $J = 6.9$ Hz, 2H), 2.20–2.10 (m, 1H), 1.93 (s, 3H), 1.89–1.87 (m, 4H), 0.90 (d, $J = 6.4$ Hz, 6H). ^{13}C NMR (DMSO): δ 206.3, 166.7, 163.0, 161.8, 150.8, 130.9, 127.2, 117.1, 114.7, 114.0, 112.5, 103.9, 69.0, 68.2, 46.5, 26.0, 25.7, 22.9, 8.0. ESI-MS m/z 419 $[\text{M} + \text{H}]^+$. HRMS m/z calcd for $\text{C}_{23}\text{H}_{27}\text{FO}_6$ $[\text{M} + \text{H}]^+$: 419.1864. Found: 419.1848.

4-[4-(2-Cyclopentylacetyl)-3-hydroxy-2-methylphenoxy]butoxy-3-fluorobenzoic Acid (43). Colorless solid (0.213 g, 48%); mp 160–162 °C. ^1H NMR (DMSO): δ 7.79 (d, $J = 9.2$ Hz, 1H), 7.70–7.76 (m, 1H), 7.60–7.58 (m, 1H), 7.22 (t, $J = 8.7$ Hz, 1H), 6.58 (d, $J = 9.2$ Hz, 1H), 4.17–4.12 (m, 4H), 2.94 (d, $J = 7.3$ Hz, 2H), 2.20–2.18 (m, 1H), 1.92 (s, 3H), 1.89–1.87 (m, 4H), 1.72–1.69 (m, 2H), 1.55–1.44 (m, 4H), 1.12–1.10 (m, 2H). ^{13}C NMR (DMSO): δ 206.3, 166.7, 162.9, 161.8, 150.8, 130.8, 127.2, 123.8, 117.0, 114.7, 113.8, 112.5, 103.8, 69.0, 68.2, 43.8, 36.8, 32.6, 25.7, 25.0, 8.0. ESI-MS m/z 445 $[\text{M} + \text{H}]^+$. HRMS m/z calcd for $\text{C}_{25}\text{H}_{29}\text{FO}_6$ $[\text{M} + \text{H}]^+$: 445.2021. Found: 445.2014.

4-[4-[3-Hydroxy-2-methyl-4-(3-methylbutanoyl)phenoxy]butoxy]-3-methoxybenzoic Acid (44). Colorless solid (0.301 g, 70%); mp 133–135 °C. ^1H NMR (DMSO): δ 7.78 (d, $J = 8.7$ Hz, 1H), 7.53–7.51 (m, 1H), 7.40 (d, $J = 1.8$ Hz, 1H), 7.00 (d, $J = 8.2$ Hz, 1H), 6.59 (d, $J = 9.2$ Hz, 1H), 4.13–4.07 (m, 4H), 3.76 (s, 3H), 2.83 (d, $J = 6.9$ Hz, 2H), 2.12–2.10 (m, 1H), 1.94 (s, 3H), 1.90–1.88 (m, 4H), 0.89 (d, $J = 6.9$ Hz, 6H). ^{13}C NMR (DMSO): δ 205.7, 167.1, 162.5, 161.3, 151.9, 148.4, 130.3, 122.9, 113.4, 111.9, 103.3, 67.9, 67.8, 55.4, 45.9, 25.4, 22.4, 7.5. ESI-MS m/z 431 $[\text{M} + \text{H}]^+$. HRMS m/z calcd for $\text{C}_{24}\text{H}_{30}\text{O}_7$ $[\text{M} + \text{H}]^+$: 431.2064. Found: 431.2061.

4-[4-(2-Cyclopentylacetyl)-3-hydroxy-2-methylphenoxy]butoxy-methoxybenzoic Acid (45). Colorless solid (0.292 g, 64%). ^1H NMR (DMSO): δ 7.80 (d, $J = 9.2$ Hz, 1H), 7.50–7.49 (m, 1H), 7.39 (d, $J = 1.8$ Hz, 1H), 7.00 (d, $J = 8.7$ Hz, 1H), 6.60 (d, $J = 9.2$ Hz, 1H), 4.14–4.07 (m, 4H), 3.75 (s, 3H), 2.95 (d, $J = 6.9$ Hz, 2H), 2.21–2.19 (m, 1H), 1.94 (s, 3H), 1.89–1.87 (m, 4H), 1.74–1.72 (m, 2H), 1.56–1.45 (m, 4H), 1.14–1.12 (m, 2H). ^{13}C NMR (DMSO): δ 205.8, 167.1, 162.4, 161.2, 151.8, 148.4, 130.3, 123.1, 113.2, 112.1, 111.9, 103.3, 67.9, 67.8, 55.5, 43.2, 36.3, 32.0, 25.5, 25.2, 24.4, 7.5. ESI-MS m/z 457 $[\text{M} + \text{H}]^+$. HRMS m/z calcd for $\text{C}_{26}\text{H}_{32}\text{O}_7$ $[\text{M} + \text{H}]^+$: 457.2221. Found: 457.2218.

3-Chloro-4-[4-[3-hydroxy-2-methyl-4-(3-methylbutanoyl)phenoxy]butoxy]benzoic Acid (46). Colorless solid (0.252 g, 58%); mp 147–149 °C. ^1H NMR (DMSO): δ 7.86–7.84 (m, 3H), 7.21 (d, $J = 8.7$ Hz, 1H), 6.61 (d, $J = 9.2$ Hz, 1H), 4.20–4.15 (m, 4H), 2.81 (d, $J = 6.9$ Hz, 2H), 2.21–2.10 (m, 1H), 1.93 (s, 3H), 1.92–1.89 (m, 4H), 0.90 (d, $J = 6.4$ Hz, 6H). ^{13}C NMR (DMSO): δ 206.0, 166.6, 163.0, 161.8, 150.7, 130.9, 127.2, 117.1, 114.9, 114.0, 112.5, 103.8, 69.0, 68.1, 46.3, 26.0, 25.8, 22.4, 8.0. ESI-MS m/z 435 $[\text{M} + \text{H}]^+$. HRMS m/z calcd for $\text{C}_{23}\text{H}_{27}\text{ClO}_6$ $[\text{M} + \text{H}]^+$: 435.1569. Found: 435.1557.

3-Chloro-4-[4-(2-cyclopentylacetyl)-3-hydroxy-2-methylphenoxy]butoxy]benzoic Acid (47). Colorless solid (0.253 g, 55%). ^1H NMR (DMSO): δ 7.87–7.82 (m, 3H), 7.23 (d, $J = 8.2$ Hz, 1H), 6.62 (d, $J = 9.2$ Hz, 1H), 4.22–4.17 (m, 4H), 2.98 (d, $J = 6.9$ Hz, 2H), 2.23–2.21 (m, 1H), 1.95 (s, 3H), 1.94–1.91 (m, 4H), 1.76–1.74 (m, 2H), 1.56–1.44 (m, 4H), 1.18–1.15 (m, 2H). ^{13}C NMR (DMSO): δ 206.0, 166.7, 162.9, 161.8, 151.0, 130.8, 127.2, 123.7, 117.0, 114.6, 113.9, 112.5, 103.8, 69.1, 68.2, 43.7, 36.8, 32.7, 25.7, 25.1, 8.0. ESI-MS m/z 461 $[\text{M} + \text{H}]^+$. HRMS m/z calcd for $\text{C}_{25}\text{H}_{29}\text{ClO}_6$ $[\text{M} + \text{H}]^+$: 461.1725. Found: 461.1720.

4-[4-[3-Hydroxy-2-methyl-4-(3-methylbutanoyl)phenoxy]butoxy]-2-methylbenzoic Acid (48). Colorless solid (0.269 g, 65%); mp 136–138 °C. ^1H NMR (DMSO): δ 7.79 (d, $J = 9.6$ Hz, 2H), 6.78–6.76 (m, 2H), 6.59 (d, $J = 9.2$ Hz, 1H), 4.11–4.06 (m, 4H), 2.80 (d, $J = 7.3$ Hz, 2H), 2.45 (s, 3H), 2.10–2.01 (m, 1H), 1.94 (s, 3H), 1.86–1.84 (m, 4H), 0.89 (d, $J = 6.9$ Hz, 6H). ^{13}C NMR (DMSO): δ 205.7, 168.0, 162.4, 161.3, 161.1, 142.1, 132.8, 130.3, 122.0, 117.2, 113.4, 111.9, 111.5, 103.3, 67.7, 67.2, 45.9, 25.3, 22.4, 21.8, 7.5. ESI-MS m/z 415 $[\text{M} + \text{H}]^+$. HRMS m/z calcd for $\text{C}_{24}\text{H}_{30}\text{O}_6$ $[\text{M} + \text{H}]^+$: 415.2115. Found: 415.2071.

4-[4-(2-Cyclopentylacetyl)-3-hydroxy-2-methylphenoxy]butoxy]-2-methylbenzoic Acid (49). Colorless solid (0.273 g, 62%). ^1H NMR (DMSO): δ 7.78 (d, $J = 9.2$ Hz, 2H), 6.77–6.76 (m, 2H), 6.58 (d, $J = 8.7$ Hz, 1H), 4.11–4.05 (m, 4H), 2.94 (d, $J = 7.3$ Hz, 2H), 2.46 (s, 3H), 2.20–2.01 (m, 1H), 1.94 (s, 3H), 1.86–1.84 (m, 4H), 1.74–1.71 (m, 2H), 1.56–1.45 (m, 4H), 1.13–1.01 (m, 2H). ^{13}C NMR (DMSO): δ 205.8, 168.0, 162.4, 161.1, 142.1, 132.8, 130.3, 129.6, 122.0, 117.2, 113.2, 111.9, 111.5, 103.3, 67.7, 67.2, 43.2, 36.3, 32.0, 25.2, 24.4, 21.8, 7.5. ESI-MS m/z 441 $[\text{M} + \text{H}]^+$. HRMS m/z calcd for $\text{C}_{26}\text{H}_{32}\text{O}_6$ $[\text{M} + \text{H}]^+$: 441.2272. Found: 441.2248.

3-[4-[3-Hydroxy-2-methyl-4-(3-methylbutanoyl)phenoxy]butoxy]-4-methoxybenzoic Acid (50). Colorless solid (0.254 g, 59%); mp 143–145 °C. ^1H NMR (DMSO): δ 7.80 (d, $J = 8.7$ Hz, 1H), 7.51 (d, $J = 8.2$ Hz, 1H), 7.41 (d, $J = 2.3$ Hz, 1H), 7.00 (d, $J = 8.7$ Hz, 1H), 6.60 (d, $J = 9.2$ Hz, 1H), 4.14–4.04 (m, 4H), 3.77 (s, 3H), 2.81 (d, $J = 6.9$ Hz, 2H), 2.10–2.01 (m, 1H), 1.95 (s, 3H), 1.88–1.84 (m, 4H), 0.90 (d, $J = 6.9$ Hz, 6H). ^{13}C NMR (DMSO): δ 205.7, 167.1, 162.5, 161.3, 152.7, 147.5, 130.3, 123.0, 113.4, 111.9, 111.1, 103.3, 67.9, 55.7, 45.9, 25.5, 22.4, 7.5. ESI-MS m/z 431 $[\text{M} + \text{H}]^+$. HRMS m/z calcd for $\text{C}_{24}\text{H}_{30}\text{O}_7$ $[\text{M} + \text{H}]^+$: 431.2064. Found: 431.2060.

3-[4-(2-Cyclopentylacetyl)-3-hydroxy-2-methylphenoxy]butoxy]-4-methoxybenzoic Acid (51). Colorless solid (0.273 g, 60%). ^1H NMR (DMSO): δ 7.80 (d, $J = 9.2$ Hz, 1H), 7.51 (d, $J = 8.2$ Hz, 1H), 7.41 (d, $J = 1.8$ Hz, 1H), 6.99 (d, $J = 8.7$ Hz, 1H), 6.60 (d, $J = 9.2$ Hz, 1H), 4.14–4.04 (m, 4H), 3.77 (s, 3H), 2.95 (d, $J = 6.9$ Hz, 2H), 2.21–2.10 (m, 1H), 1.94 (s, 3H), 1.88–1.84 (m, 4H), 1.72–1.69 (m, 2H), 1.56–1.45 (m, 4H), 1.14–1.12 (m, 2H). ^{13}C NMR (DMSO): δ 205.8, 167.1, 162.4, 161.2, 152.7, 147.5, 130.3, 123.1, 113.2, 111.9, 111.1, 103.3, 67.9, 55.7, 43.2, 36.3, 32.0, 25.4, 24.4, 7.5. ESI-MS m/z 457 $[\text{M} + \text{H}]^+$. HRMS m/z calcd for $\text{C}_{26}\text{H}_{32}\text{O}_7$ $[\text{M} + \text{H}]^+$: 457.2221. Found: 457.2224.

4-(4-(4-Acetyl-3-hydroxy-2-methylphenoxy)butoxy)-3-methoxybenzoic Acid (52). Colorless solid (0.255 g, 58%); mp 138–140 °C. ^1H NMR (DMSO): δ 7.75 (d, $J = 9.2$ Hz, 1H), 7.48 (d, $J = 8.2$ Hz, 1H), 7.39 (s, 1H), 7.02 (d, $J = 8.2$ Hz, 1H), 6.62 (d, $J = 8.7$ Hz, 1H), 4.13–4.07 (m, 4H), 3.75 (s, 3H), 2.53 (s, 3H), 1.93 (s, 3H), 1.89–1.87 (m, 4H). ^{13}C NMR (DMSO): δ 204.4, 167.7, 163.1, 161.5, 152.3, 148.9, 131.4, 123.6, 11.0, 112.6, 112.4, 112.3, 103.9, 68.5, 68.3, 55.9, 26.9, 26.0, 25.7, 8.0. LC–MS (ESI) calcd for $\text{C}_{21}\text{H}_{24}\text{O}_7$ $[\text{M} + \text{H}]^+$: 389.15. Found: 389.05. HRMS (ESI) calcd for $\text{C}_{21}\text{H}_{24}\text{O}_7$ $[\text{M} + \text{H}]^+$: 389.1595. Found: 389.1587.

3-(4-(4-Acetyl-3-hydroxy-2-methylphenoxy)butoxy)-4-methoxybenzoic Acid (53). Colorless solid (0.264 g, 68%); mp 135–136 °C. ^1H NMR (DMSO): δ 7.76 (d, $J = 9.2$ Hz, 1H), 7.50 (d, $J = 10.0$ Hz, 1H), 7.42 (s, 1H), 6.99 (d, $J = 8.7$ Hz, 1H), 6.60 (d, $J = 9.2$ Hz, 1H), 4.13–4.03 (m, 4H), 3.77 (s, 3H), 2.53 (s, 3H), 1.94 (s, 3H), 1.92–1.88 (m, 4H). ^{13}C NMR (DMSO): δ 204.3, 167.6, 163.1, 161.5, 153.3, 148.0, 131.4, 123.7, 123.5, 114.0, 113.7, 112.3, 111.7, 103.9, 68.4, 56.2, 26.8, 25.9, 8.0. LC–MS (ESI) calcd for $\text{C}_{21}\text{H}_{24}\text{O}_7$ $[\text{M} + \text{H}]^+$: 389.15. Found: 389.00. HRMS (ESI) calcd for $\text{C}_{21}\text{H}_{24}\text{O}_7$ $[\text{M} + \text{H}]^+$: 389.1595. Found: 389.1585.

3-(4-(4-Acetyl-3-hydroxy-2-methylphenoxy)butoxy)-2-methylbenzoic Acid (54). Colorless solid (0.204 g, 55%); mp 140–142 °C. ^1H NMR (DMSO): δ 7.73 (d, $J = 9.2$ Hz, 1H), 7.27 (d, $J = 8.7$ Hz, 1H), 7.16 (t, $J = 7.8$ Hz, 1H), 7.16 (d, $J = 7.8$ Hz, 1H), 6.58 (d, $J = 8.7$ Hz, 1H), 4.11–4.02 (m, 4H), 2.52 (s, 3H), 2.28 (s, 3H), 1.93 (s, 3H), 1.89–1.87 (m, 4H). ^{13}C NMR (DMSO): δ 204.3, 169.7, 163.0, 161.5, 157.4, 133.2, 131.4, 127.1, 126.7, 121.9, 114.8, 114.0, 112.3, 103.8, 68.3, 68.1, 26.8, 25.9, 13.1, 8.0. LC–MS (ESI) calcd for $\text{C}_{21}\text{H}_{24}\text{FO}_6$ $[\text{M} + \text{H}]^+$: 373.16. Found: 373.00. HRMS (ESI) calcd for $\text{C}_{21}\text{H}_{24}\text{O}_6$ $[\text{M} + \text{Na}]^+$: 395.1465. Found: 395.1464.

5-(4-(4-Acetyl-3-hydroxy-2-methylphenoxy)butoxy)-2-fluorobenzoic Acid (55). Colorless solid (0.229 g, 0.253 g, 61%); mp 102–104 °C. ^1H NMR (DMSO): δ 7.75 (d, $J = 8.7$ Hz, 1H), 7.26–7.13 (m, 3H), 6.59 (d, $J = 9.2$ Hz, 1H), 4.11–4.03 (m, 4H), 2.52 (s, 3H), 1.94 (s, 3H), 1.92–1.86 (m, 4H). ^{13}C NMR (DMSO): δ 204.3, 165.4, 163.0, 161.5, 154.8, 154.6, 131.4, 118.4, 118.2, 116.5, 114.0, 112.3, 103.8, 68.3, 26.9, 25.8, 8.0. LC–MS (ESI) calcd for $\text{C}_{20}\text{H}_{21}\text{FO}_6$ $[\text{M} + \text{H}]^+$: 377.13. Found: 377.00. HRMS (ESI) calcd for $\text{C}_{20}\text{H}_{21}\text{FO}_6$ $[\text{M} + \text{H}]^+$: 377.1395. Found: 377.1395.

4-(4-(4-Acetyl-3-hydroxy-2-methylphenoxy)butoxy)-3-methylbenzoic Acid (56). Colorless solid (0.201 g, 54%); mp 188–190 °C. ^1H NMR (DMSO): δ 7.70–7.65 (m, 2H), 7.64 (s, 1H), 6.93 (d, J = 8.7 Hz, 1H), 6.57 (d, J = 9.2 Hz, 1H), 4.09–4.04 (m, 4H), 2.49 (s, 3H), 2.08 (s, 3H), 1.89 (s, 3H), 1.88–1.86 (m, 4H). ^{13}C NMR (DMSO): δ 204.4, 167.7, 163.0, 161.5, 160.8, 132.0, 131.4, 129.7, 126.2, 122.8, 114.0, 112.3, 112.2, 108.8, 68.3, 67.9, 26.8, 25.9, 25.8, 16.4, 8.0. LC–MS (ESI) calcd for $\text{C}_{21}\text{H}_{24}\text{O}_6$ $[\text{M} + \text{H}]^+$: 373.16. Found: 373.00. HRMS (ESI) calcd for $\text{C}_{21}\text{H}_{24}\text{O}_6$ $[\text{M} + \text{Na}]^+$: 395.1465. Found: 395.1463.

4-(4-(3-Hydroxy-2-methyl-4-propionylphenoxy)butoxy)-3-methoxybenzoic Acid (57). Colorless solid (0.253 g, 63%); mp 128–130 °C. ^1H NMR (DMSO): δ 7.80 (d, J = 9.2 Hz, 1H), 7.49 (d, J = 8.2 Hz, 1H), 7.40 (s, 1H), 7.01 (d, J = 8.7 Hz, 1H), 6.60 (d, J = 9.2 Hz, 1H), 4.13–4.03 (m, 4H), 3.74 (s, 3H), 2.99 (q, J = 7.5 Hz, 2H), 1.96 (s, 3H), 1.90–1.88 (m, 4H), 1.07 (t, J = 7.3 Hz, 3H). ^{13}C NMR (DMSO): δ 206.8, 162.9, 161.5, 152.3, 148.9, 130.5, 123.6, 113.5, 112.6, 112.4, 103.9, 98.5, 68.5, 66.9, 66.2, 60.6, 60.0, 31.1, 26.0, 25.7, 8.9, 8.0. LC–MS (ESI) calcd for $\text{C}_{22}\text{H}_{26}\text{O}_7$ $[\text{M} + \text{H}]^+$: 403.17. Found: 403.00. HRMS (ESI) calcd for $\text{C}_{22}\text{H}_{26}\text{O}_7$ $[\text{M} + \text{Na}]^+$: 425.1571. Found: 425.1568.

3-(4-(3-Hydroxy-2-methyl-4-propionylphenoxy)butoxy)-4-methoxybenzoic Acid (58). Colorless solid (0.293 g, 73%); mp 120–122 °C. ^1H NMR (DMSO): δ 7.77 (d, J = 8.6 Hz, 1H), 7.50 (d, J = 10.5 Hz, 1H), 7.42 (s, 1H), 6.99 (d, J = 8.7 Hz, 1H), 6.60 (d, J = 9.1 Hz, 1H), 4.13–4.03 (m, 4H), 3.77 (s, 3H), 2.98 (q, J = 7.5 Hz, 2H), 1.95 (s, 3H), 1.90–1.88 (m, 4H), 1.05 (t, J = 7.3 Hz, 3H). ^{13}C NMR (DMSO): δ 206.8, 167.7, 162.9, 161.5, 153.3, 148.0, 130.4, 123.7, 113.7, 113.4, 112.4, 111.6, 103.8, 68.5, 68.4, 56.2, 30.6, 25.5, 25.4, 8.9, 8.0. LC–MS (ESI) calcd for $\text{C}_{22}\text{H}_{26}\text{O}_7$ $[\text{M} + \text{H}]^+$: 403.17. Found: 403.35. HRMS (ESI) calcd for $\text{C}_{22}\text{H}_{26}\text{O}_7$ $[\text{M} + \text{Na}]^+$: 425.1571. Found: 425.1569.

3-(4-(3-Hydroxy-2-methyl-4-propionylphenoxy)butoxy)-2-methylbenzoic Acid (59). Colorless solid (0.228 g, 59%); mp 103–105 °C. ^1H NMR (DMSO): δ 7.77 (d, J = 9.2 Hz, 1H), 7.24 (d, J = 9.2 Hz, 1H), 7.16 (t, J = 7.8 Hz, 1H), 7.08 (d, J = 8.2 Hz, 1H), 6.59 (d, J = 9.2 Hz, 1H), 4.12–4.02 (m, 4H), 3.00 (q, J = 7.3 Hz, 2H), 2.28 (s, 3H), 1.94 (s, 3H), 1.90–1.89 (m, 4H), 1.05 (t, J = 7.4 Hz, 3H). ^{13}C NMR (DMSO): δ 206.8, 169.7, 162.8, 161.5, 157.4, 133.2, 130.4, 127.1, 126.8, 121.9, 114.8, 113.5, 112.4, 103.8, 63.3, 31.8, 24.6, 13.1, 8.9, 8.0. LC–MS (ESI) calcd for $\text{C}_{22}\text{H}_{26}\text{O}_6$ $[\text{M} + \text{H}]^+$: 387.17. Found: 387.05. HRMS (ESI) calcd for $\text{C}_{22}\text{H}_{26}\text{O}_6$ $[\text{M} + \text{H}]^+$: 387.1802. Found: 387.1802.

2-Fluoro-5-(4-(3-hydroxy-2-methyl-4-propionylphenoxy)butoxy)benzoic Acid (60). Colorless solid (0.254 g, 65%); mp 123–125 °C. ^1H NMR (DMSO): δ 7.76 (d, J = 8.7 Hz, 1H), 7.26–7.13 (m, 3H), 6.59 (d, J = 9.2 Hz, 1H), 4.11–4.02 (m, 4H), 2.98 (q, J = 7.3 Hz, 2H), 1.93 (s, 3H), 1.90–1.86 (m, 4H), 1.05 (t, J = 7.3 Hz, 3H). ^{13}C NMR (DMSO): δ 206.8, 165.5, 162.8, 161.5, 154.8, 154.6, 130.4, 118.4, 116.5, 113.5, 112.4, 103.8, 68.3, 31.1, 25.8, 8.9, 8.0. LC–MS (ESI) calcd for $\text{C}_{21}\text{H}_{23}\text{FO}_6$ $[\text{M} + \text{H}]^+$: 391.15. Found: 391.00. HRMS (ESI) calcd for $\text{C}_{21}\text{H}_{23}\text{FO}_6$ $[\text{M} + \text{Na}]^+$: 413.1371. Found: 413.1366.

4-(4-(3-Hydroxy-2-methyl-4-propionylphenoxy)butoxy)-3-methylbenzoic Acid (61). Colorless solid (0.205 g, 53%); mp 178–180 °C. ^1H NMR (DMSO): δ 7.80–7.78 (m, 2H), 7.70 (s, 1H), 6.99 (d, J = 8.7 Hz, 1H), 6.63 (d, J = 9.2 Hz, 1H), 4.15–4.10 (m, 4H), 3.02 (q, J = 7.3 Hz, 2H), 2.24 (s, 3H), 1.96 (s, 3H), 1.95–1.92 (m, 4H), 1.08 (t, J = 7.3 Hz, 3H). ^{13}C NMR (DMSO): δ 206.8, 167.7, 162.8, 161.5, 160.8, 132.0, 130.5, 129.7, 126.2, 122.8, 113.5, 112.4, 111.2, 103.8, 68.3, 67.9, 31.1, 25.9, 25.8, 16.4, 8.9, 8.0. LC–MS (ESI) calcd for $\text{C}_{22}\text{H}_{26}\text{O}_6$ $[\text{M} + \text{H}]^+$: 387.17. Found: 387.05. HRMS (ESI) calcd for $\text{C}_{22}\text{H}_{26}\text{O}_6$ $[\text{M} + \text{Na}]^+$: 409.1622. Found: 409.1625.

4-(4-(3-Hydroxy-4-isobutyl-2-methylphenoxy)butoxy)-3-methoxybenzoic Acid (62). Colorless solid (0.283 g, 68%); mp 118–120 °C. ^1H NMR (DMSO): δ 7.84 (d, J = 8.7 Hz, 1H), 7.49 (d, J = 10.5 Hz, 1H), 7.39 (s, 1H), 7.00 (d, J = 8.2 Hz, 1H), 6.61 (d, J = 9.2 Hz, 1H), 4.14–4.07 (m, 4H), 3.74 (s, 3H), 3.74–3.63 (m, 1H), 1.94 (s, 3H), 1.90–1.88 (m, 4H), 1.09 (d, J = 6.9 Hz, 6H). ^{13}C NMR (DMSO): δ 210.3, 167.6, 163.0, 162.3, 152.4, 148.9, 130.5, 123.6, 123.5, 112.7, 112.6, 112.4, 112.2, 103.9, 68.5, 56.0, 34.8, 26.0, 25.7,

20.0, 8.1. LC–MS (ESI) calcd for $\text{C}_{23}\text{H}_{28}\text{O}_7$ $[\text{M} + \text{H}]^+$: 417.18. Found: 417.05. HRMS (ESI) calcd for $\text{C}_{23}\text{H}_{28}\text{O}_7$ $[\text{M} + \text{Na}]^+$: 439.1727. Found: 439.1725.

3-(4-(3-Hydroxy-4-isobutyl-2-methylphenoxy)butoxy)-4-methoxybenzoic Acid (63). Colorless solid (0.279 g, 67%); mp 82–84 °C. ^1H NMR (DMSO): δ 7.84 (d, J = 9.2 Hz, 1H), 7.50 (d, J = 10.5 Hz, 1H), 7.42 (s, 1H), 6.99 (d, J = 8.7 Hz, 1H), 6.61 (d, J = 9.2 Hz, 1H), 4.14 (brs, 2H), 4.07 (brs, 2H), 3.77 (s, 3H), 3.74–3.63 (m, 1H), 1.95 (s, 3H), 1.88 (brs, 4H), 1.08 (d, J = 6.4 Hz, 6H). ^{13}C NMR (DMSO): δ 210.2, 167.6, 163.0, 162.3, 153.3, 148.1, 130.4, 123.7, 113.7, 112.7, 112.2, 111.7, 103.9, 68.4, 56.2, 26.0, 19.9, 8.1. LC–MS (ESI) calcd for $\text{C}_{23}\text{H}_{28}\text{O}_7$ $[\text{M} + \text{H}]^+$: 417.18. Found: 417.05. HRMS (ESI) calcd for $\text{C}_{23}\text{H}_{28}\text{O}_7$ $[\text{M} + \text{H}]^+$: 417.1908. Found: 417.1895.

3-(4-(3-Hydroxy-4-isobutyl-2-methylphenoxy)butoxy)-2-methylbenzoic Acid (64). Colorless solid (0.264 g, 66%); mp 115–117 °C. ^1H NMR (DMSO): δ 7.85 (d, J = 9.2 Hz, 1H), 7.28 (d, J = 6.8 Hz, 1H), 7.18 (t, J = 7.8 Hz, 1H), 7.10 (d, J = 7.3 Hz, 1H), 6.64 (d, J = 9.2 Hz, 1H), 4.16–4.05 (m, 4H), 3.66–3.54 (m, 1H), 2.03 (s, 3H), 1.93 (s, 3H), 1.91–1.88 (m, 4H), 1.10 (d, J = 6.8 Hz, 6H). ^{13}C NMR (DMSO): δ 210.2, 169.7, 162.9, 157.4, 133.2, 130.4, 127.1, 126.8, 121.9, 114.8, 112.7, 112.2, 103.9, 68.3, 68.1, 34.3, 26.0, 19.9, 13.1, 8.0. LC–MS (ESI) calcd for $\text{C}_{23}\text{H}_{28}\text{O}_6$ $[\text{M} + \text{H}]^+$: 401.19. Found: 401.05. HRMS (ESI) calcd for $\text{C}_{23}\text{H}_{28}\text{O}_6$ $[\text{M} + \text{H}]^+$: 401.1959. Found: 401.1948.

2-Fluoro-5-(4-(3-hydroxy-4-isobutyl-2-methylphenoxy)butoxy)benzoic Acid (65). Colorless solid (0.234 g, 58%); mp 122–124 °C. ^1H NMR (DMSO): δ 7.82 (d, J = 9.2 Hz, 1H), 7.27–7.13 (m, 3H), 6.61 (d, J = 8.7 Hz, 1H), 4.12–4.02 (m, 4H), 3.64–3.46 (m, 1H), 1.94 (s, 3H), 1.90–1.86 (m, 4H), 1.08 (d, J = 6.9 Hz, 6H). ^{13}C NMR (DMSO): δ 210.2, 165.5, 162.9, 162.3, 154.8, 154.6, 130.5, 118.2, 116.4, 112.7, 112.2, 103.9, 68.3, 33.6, 25.8, 19.9, 8.0. LC–MS (ESI) calcd for $\text{C}_{22}\text{H}_{25}\text{FO}_6$ $[\text{M} + \text{H}]^+$: 405.16. Found: 405.00. HRMS (ESI) calcd for $\text{C}_{22}\text{H}_{25}\text{FO}_6$ $[\text{M} + \text{H}]^+$: 405.1708. Found: 405.1705.

4-(4-(3-Hydroxy-4-isobutyl-2-methylphenoxy)butoxy)-3-methylbenzoic Acid (66). Colorless solid (0.224 g, 56%); mp 160–162 °C. ^1H NMR (DMSO): δ 7.84 (d, J = 9.2 Hz, 1H), 7.75–7.71 (m, 1H), 7.76 (s, 1H), 6.98 (d, J = 8.7 Hz, 1H), 6.61 (d, J = 9.2 Hz, 1H), 4.14–4.09 (m, 4H), 3.71–3.61 (m, 1H), 2.12 (s, 3H), 1.94 (s, 3H), 1.94–1.90 (m, 4H), 1.08 (d, J = 5.5 Hz, 6H). ^{13}C NMR (DMSO): δ 210.2, 167.7, 162.9, 162.3, 160.8, 132.0, 130.5, 129.7, 126.2, 122.8, 112.7, 112.3, 111.2, 103.9, 68.3, 67.9, 34.6, 25.9, 19.9, 16.4, 8.0. LC–MS (ESI) calcd for $\text{C}_{23}\text{H}_{28}\text{O}_6$ $[\text{M} + \text{H}]^+$: 401.19. Found: 401.05. HRMS (ESI) calcd for $\text{C}_{23}\text{H}_{28}\text{O}_6$ $[\text{M} + \text{Na}]^+$: 423.1778. Found: 423.1778.

4-(4-(4-Butyl-3-hydroxy-2-methylphenoxy)butoxy)-3-methoxybenzoic Acid (67). Colorless solid (0.270 g, 65%); mp 148–150 °C. ^1H NMR (DMSO): δ 7.80 (d, J = 9.2 Hz, 1H), 7.48 (d, J = 10.5 Hz, 1H), 7.39 (s, 1H), 7.00 (d, J = 8.2 Hz, 1H), 6.60 (d, J = 8.7 Hz, 1H), 4.13–4.07 (m, 4H), 3.75 (s, 3H), 2.93 (t, J = 7.5 Hz, 2H), 1.94 (s, 3H), 1.91–1.88 (m, 4H), 1.61–1.57 (m, 2H), 0.90 (t, J = 7.3 Hz, 3H). ^{13}C NMR (DMSO): δ 206.4, 167.4, 162.9, 161.7, 152.4, 148.9, 130.7, 123.6, 123.5, 112.5, 112.4, 103.8, 68.5, 68.3, 55.9, 26.0, 25.7, 18.4, 14.1, 8.0. LC–MS (ESI) calcd for $\text{C}_{23}\text{H}_{28}\text{O}_7$ $[\text{M} + \text{H}]^+$: 417.18. Found: 417.00. HRMS (ESI) calcd for $\text{C}_{23}\text{H}_{28}\text{O}_7$ $[\text{M} + \text{H}]^+$: 417.1908. Found: 417.1903.

3-(4-(4-Butyl-3-hydroxy-2-methylphenoxy)butoxy)-4-methoxybenzoic Acid (68). Colorless solid (0.279 g, 67%); mp 129–131 °C. ^1H NMR (DMSO): δ 7.79 (d, J = 9.1 Hz, 1H), 7.43 (d, J = 10.0 Hz, 1H), 7.43 (s, 1H), 7.02 (d, J = 8.7 Hz, 1H), 6.63 (d, J = 9.2 Hz, 1H), 4.13–4.07 (m, 4H), 3.79 (s, 3H), 2.99 (t, J = 7.3 Hz, 2H), 1.96 (s, 3H), 1.89–1.86 (m, 4H), 1.63–1.61 (m, 2H), 0.92 (d, J = 7.6 Hz, 3H). ^{13}C NMR (DMSO): δ 206.4, 167.6, 162.9, 161.7, 153.3, 148.0, 130.6, 123.7, 123.4, 113.6, 112.4, 111.6, 103.8, 68.44, 68.41, 56.2, 26.0, 25.6, 18.4, 14.1, 8.0. LC–MS (ESI) calcd for $\text{C}_{23}\text{H}_{28}\text{O}_7$ $[\text{M} + \text{H}]^+$: 417.18. Found: 417.00. HRMS (ESI) calcd for $\text{C}_{23}\text{H}_{28}\text{O}_7$ $[\text{M} + \text{H}]^+$: 417.1908. Found: 417.1896.

3-(4-(4-Butyl-3-hydroxy-2-methylphenoxy)butoxy)-2-methylbenzoic Acid (69). Colorless solid (0.244 g, 61%); mp 97–99 °C. ^1H NMR (DMSO): δ 7.78 (d, J = 8.7 Hz, 1H), 7.27 (d, J = 7.3 Hz, 1H), 7.17 (t, J = 8.2 Hz, 1H), 7.08 (d, J = 7.8 Hz, 1H), 6.59 (d,

$J = 9.2$ Hz, 1H), 4.13–4.02 (m, 4H), 2.92 (t, $J = 7.3$ Hz, 2H), 2.28 (s, 3H), 1.94 (s, 3H), 1.89–1.86 (m, 4H), 1.61–1.57 (m, 2H), 0.89 (t, $J = 7.8$ Hz, 3H). ^{13}C NMR (DMSO): δ 206.4, 169.6, 162.9, 161.7, 157.4, 133.1, 130.6, 127.1, 126.8, 121.8, 114.8, 113.7, 112.5, 103.8, 68.3, 68.2, 26.0, 18.4, 14.1, 13.1, 8.0. LC–MS (ESI) calcd for $\text{C}_{23}\text{H}_{28}\text{O}_6$ $[\text{M} + \text{H}]^+$: 401.19. Found: 401.05. HRMS (ESI) calcd for $\text{C}_{23}\text{H}_{28}\text{O}_6$ $[\text{M} + \text{Na}]^+$: 439.1727. Found: 439.1727.

5-(4-(4-Butyryl-3-hydroxy-2-methylphenoxy)butoxy)-2-fluorobenzoic Acid (70). Colorless solid (0.255 g, 63%); mp 88–90 °C. ^1H NMR (DMSO): δ 7.78 (d, $J = 8.7$ Hz, 1H), 7.27–7.13 (m, 3H), 6.59 (d, $J = 9.2$ Hz, 1H), 4.11–4.02 (m, 4H), 2.92 (t, $J = 7.3$ Hz, 2H), 1.94 (s, 3H), 1.89–1.87 (m, 4H), 1.61–1.59 (m, 2H), 0.89 (t, $J = 7.3$ Hz, 3H). ^{13}C NMR (DMSO): δ 206.4, 165.4, 162.9, 161.7, 154.8, 154.6, 130.6, 118.2, 116.4, 113.6, 112.4, 103.8, 68.3, 25.8, 18.3, 14.1, 8.0. LC–MS (ESI) calcd for $\text{C}_{22}\text{H}_{25}\text{FO}_6$ $[\text{M} + \text{H}]^+$: 405.43. Found: 405.05. HRMS (ESI) calcd for $\text{C}_{22}\text{H}_{25}\text{FO}_6$ $[\text{M} + \text{Na}]^+$: 427.1527. Found: 427.1523.

4-(4-(4-Butyryl-3-hydroxy-2-methylphenoxy)butoxy)-3-methylbenzoic Acid (71). Colorless solid (0.232 g, 58%); mp 161–163 °C. ^1H NMR (DMSO): δ 7.79 (d, $J = 9.2$ Hz, 1H), 7.71 (d, $J = 8.7$ Hz, 1H), 7.68 (s, 1H), 6.97 (d, $J = 8.7$ Hz, 1H), 6.59 (d, $J = 8.7$ Hz, 1H), 4.13–4.08 (m, 4H), 2.92 (t, $J = 7.3$ Hz, 2H), 2.12 (s, 3H), 1.94 (s, 3H), 1.90–1.88 (m, 4H), 1.63–1.61 (m, 2H), 0.89 (t, $J = 7.3$ Hz, 3H). ^{13}C NMR (DMSO): δ 206.4, 167.7, 162.9, 161.7, 160.8, 132.0, 130.7, 129.7, 126.3, 122.8, 113.7, 112.5, 111.2, 103.9, 68.3, 67.9, 26.1, 25.9, 18.4, 16.3, 14.1, 8.0. LC–MS (ESI) calcd for $\text{C}_{23}\text{H}_{28}\text{O}_6$ $[\text{M} + \text{H}]^+$: 401.19. Found: 401.05. HRMS (ESI) calcd for $\text{C}_{23}\text{H}_{28}\text{O}_6$ $[\text{M} + \text{Na}]^+$: 423.1778. Found: 423.1778.

3-(4-(4-(3,3-Dimethylbutanoyl)-3-hydroxy-2-methylphenoxy)butoxy)-4-methoxybenzoic Acid (72). Colorless solid (0.270 g, 61%); mp 140–142 °C. ^1H NMR (DMSO): δ 7.84 (d, $J = 9.2$ Hz, 1H), 7.50 (d, $J = 10.0$ Hz, 1H), 7.49 (s, 1H), 7.00 (d, $J = 8.7$ Hz, 1H), 6.58 (d, $J = 9.2$ Hz, 1H), 4.13–4.03 (m, 4H), 3.79 (s, 3H), 2.80 (s, 2H), 1.94 (s, 3H), 1.89–1.87 (m, 4H), 0.96 (s, 9H). ^{13}C NMR (DMSO): δ 206.4, 167.6, 163.1, 162.1, 153.3, 148.1, 131.8, 123.7, 123.5, 114.9, 113.6, 111.6, 103.6, 68.4, 56.2, 49.1, 32.1, 30.5, 26.0, 25.8, 8.0. LC–MS (ESI) calcd for $\text{C}_{25}\text{H}_{32}\text{O}_7$ $[\text{M} + \text{H}]^+$: 445.21. Found: 445.00. HRMS (ESI) calcd for $\text{C}_{25}\text{H}_{32}\text{O}_7$ $[\text{M} + \text{Na}]^+$: 467.2040. Found: 467.2041.

4-(4-(4-(3,3-Dimethylbutanoyl)-3-hydroxy-2-methylphenoxy)butoxy)-5-methoxycyclohexa-1,3-dienecarboxylic Acid (73). Colorless solid (0.258 g, 58%); mp 133–135 °C. ^1H NMR (DMSO): δ 7.86 (d, $J = 9.2$ Hz, 1H), 7.48 (d, $J = 10.1$ Hz, 1H), 7.39 (s, 1H), 7.01 (d, $J = 8.7$ Hz, 1H), 6.58 (d, $J = 9.2$ Hz, 1H), 4.13–4.07 (m, 4H), 3.77 (s, 3H), 2.80 (s, 2H), 1.94 (s, 3H), 1.89–1.87 (m, 4H), 0.96 (s, 9H). ^{13}C NMR (DMSO): δ 206.4, 167.6, 163.1, 162.1, 152.4, 148.9, 131.8, 123.6, 114.9, 112.6, 112.4, 103.6, 68.4, 55.9, 49.1, 32.1, 30.5, 26.0, 25.8, 8.0. LC–MS (ESI) calcd for $\text{C}_{25}\text{H}_{32}\text{O}_7$ $[\text{M} + \text{H}]^+$: 445.21. Found: 445.00. HRMS (ESI) calcd for $\text{C}_{25}\text{H}_{32}\text{O}_7$ $[\text{M} + \text{Na}]^+$: 467.2040. Found: 467.2045.

3-(4-(4-(3,3-Dimethylbutanoyl)-3-hydroxy-2-methylphenoxy)butoxy)-2-methylbenzoic Acid (74). Colorless solid (0.278 g, 65%); mp 123–125 °C. ^1H NMR (DMSO): δ 7.84 (d, $J = 8.7$ Hz, 1H), 7.26 (d, $J = 7.8$ Hz, 1H), 7.16 (t, $J = 8.2$ Hz, 1H), 7.08 (d, $J = 7.3$ Hz, 1H), 6.58 (d, $J = 9.2$ Hz, 1H), 4.13–4.02 (m, 4H), 2.80 (s, 2H), 2.28 (s, 3H), 1.94 (s, 3H), 1.90–1.87 (m, 4H), 0.96 (s, 9H). ^{13}C NMR (DMSO): δ 206.4, 169.7, 163.0, 162.1, 157.4, 131.1, 131.8, 127.1, 126.8, 121.9, 114.9, 114.8, 112.4, 103.6, 68.3, 66.8, 49.1, 32.1, 30.4, 13.1, 8.0. LC–MS (ESI) calcd for $\text{C}_{25}\text{H}_{32}\text{O}_7$ $[\text{M} + \text{H}]^+$: 429.22. Found: 429.00. HRMS (ESI) calcd for $\text{C}_{25}\text{H}_{32}\text{O}_6$ $[\text{M} + \text{Na}]^+$: 451.2091. Found: 451.2093.

5-(4-(4-(3,3-Dimethylbutanoyl)-3-hydroxy-2-methylphenoxy)butoxy)-2-fluorobenzoic Acid (75). Colorless solid (0.258 g, 60%); mp 130–132 °C. ^1H NMR (DMSO): δ 7.83 (d, $J = 9.2$ Hz, 1H), 7.27–7.13 (m, 3H), 6.57 (d, $J = 9.2$ Hz, 1H), 4.11–4.02 (m, 4H), 2.79 (s, 2H), 1.94 (s, 3H), 1.86–1.85 (m, 4H), 0.96 (s, 9H). ^{13}C NMR (DMSO): δ 206.4, 165.5, 163.0, 162.1, 154.8, 154.6, 131.7, 121.2, 118.5, 116.4, 114.9, 112.4, 103.6, 68.4, 66.8, 49.1, 32.2, 30.4, 8.0. LC–MS (ESI) calcd for $\text{C}_{24}\text{H}_{29}\text{FO}_6$ $[\text{M} + \text{H}]^+$: 433.19. Found: 433.00.

HRMS (ESI) calcd for $\text{C}_{24}\text{H}_{29}\text{FO}_6$ $[\text{M} + \text{Na}]^+$: 455.1840. Found: 455.1840.

mGlu receptor in Vitro Assays. Human embryonic kidney (HEK-293) cell lines coexpressing rat mGlu receptors 2, 3, 4, 6, 7, or 8 and G protein-coupled inwardly rectifying potassium (GIRK) channels⁵⁵ were grown in growth medium containing 45% DMEM, 45% F-12, 10% FBS, 20 mM HEPES, 2 mM L-glutamine, antibiotic/antimycotic, nonessential amino acids, 700 $\mu\text{g}/\text{mL}$ G418, and 0.6 $\mu\text{g}/\text{mL}$ puromycin at 37 °C in the presence of 5% CO_2 . Cells expressing rat mGlu₁ and mGlu₅ receptor were cultured as described in Hemstapat et al.⁵⁶ All cell culture reagents were purchased from Invitrogen Corp. (Carlsbad, CA) unless otherwise noted. Calcium assays were used to assess activity of compounds at mGlu₁ and mGlu₅, as previously described by Engers et al.⁵⁷ Calcium assays at mGlu₃ were performed as described for mGlu₅ with the exception that TREx293 mGlu₃ G_{α15} cells were treated with tetracycline at 20 ng/mL for 20 h prior to assay.

Compound activity at group II (mGlu₂ and mGlu₃) and group III (mGlu₄, mGlu₆, mGlu₇, and mGlu₈) was assessed using thallium flux through GIRK channels, a method that has been described in detail.⁵⁵ Briefly, cells were plated into 384-well, black-walled, clear-bottomed poly-D-lysine-coated plates at a density of (15 000 cells/20 μL)/well in DMEM containing 10% dialyzed FBS, 20 mM HEPES, and 100 units/mL penicillin/streptomycin (assay medium). Plated cells were incubated overnight at 37 °C in the presence of 5% CO_2 . The following day, the medium was exchanged from the cells to assay buffer [Hanks' balanced salt solution (Invitrogen) containing 20 mM HEPES, pH 7.3] using an ELX405 microplate washer (BioTek), leaving 20 μL /well, followed by the addition of 20 μL /well FluoZin2-AM (330 nM final concentration) indicator dye (Invitrogen, prepared as a stock in DMSO and mixed in a 1:1 ratio with Pluronic acid F-127) in assay buffer. Cells were incubated for 1 h at room temperature, and the dye was exchanged to assay buffer using an ELX405, leaving 20 μL /well. Test compounds were diluted to 2 times their final desired concentration in assay buffer (0.3% DMSO final concentration). Agonists were diluted in thallium buffer [125 mM sodium bicarbonate (added fresh on the morning of the experiment), 1 mM magnesium sulfate, 1.8 mM calcium sulfate, 5 mM glucose, 12 mM thallium sulfate, and 10 mM HEPES, pH 7.3] at 5 times the final concentration to be assayed. Cell plates and compound plates were loaded onto a kinetic imaging plate reader (FDSS 6000 or 7000; Hamamatsu Corporation, Bridgewater, NJ). Appropriate baseline readings were taken (10 images at 1 Hz; excitation, 470 ± 20 nm; emission, 540 ± 30 nm), and test compounds were added in a 20 μL volume and incubated for approximately 2.5 min before the addition of 10 μL of thallium buffer with or without agonist. After the addition of agonist, data were collected for approximately an additional 2.5 min. Data were analyzed using Excel (Microsoft Corp, Redmond, WA). The slope of the fluorescence increase beginning 5 s after thallium/agonist addition and ending 15 s after thallium/agonist addition was calculated, corrected to vehicle and maximal agonist control slope values, and plotted using either XLfit (ID Business Solutions Ltd.) or Prism software (GraphPad Software, San Diego, CA) to generate concentration–response curves. Potencies were calculated from fits using a four-point parameter logistic equation. For concentration–response curve experiments, compounds were serially diluted 1:3 into 10 point concentration–response curves and were transferred to daughter plates using an Echo acoustic plate reformatter (Labcyte, Sunnyvale, CA). Test compounds were applied and followed by EC₂₀ concentrations of glutamate. For selectivity experiments, full concentration–response curves of glutamate or L-AP4 (for mGlu₇) were obtained in the presence of a 10 μM concentration of compound, and compounds that affected the concentration–response by less than 2-fold in terms of potency or efficacy were designated as inactive.

TREx293 mGlu₃ G_{α15} Cell Line Creation. In order to generate a tetracycline (Tet) inducible rat mGlu₃ stable cell line to be used for a calcium mobilization assay, TREx293 cells (Invitrogen) were transfected with mouse G_{α15}-pCMV6 plasmid (Origene) using Fugene6 (Promega). The cells were selected for G_{α15} expression with 1 mg/mL G418 in the presence of 10 $\mu\text{g}/\text{mL}$ blasticidin to maintain Tet repressor expression. Two weeks after the selection, polyclonal TREx293 G_{α15} cells were

obtained. The entire coding sequence of rat mGlu₃ was amplified by polymerase chain reaction (PCR) and cloned into the Tet-inducible expression plasmid pcDNA5/TO (Invitrogen). Rat mGlu₃-pcDNA5/TO was transfected into TReX293 G₄₁₅ cells and selected for mGlu₃ expression with 200 µg/mL hygromycin in the presence of G418 and blasticidins. The resulting polyclonal TReX293 mGlu₃ G₄₁₅ cells were plated for monoclonal selection, and positive monoclonal cells were identified in the calcium mobilization assay. Cells were maintained in growth medium containing DMEM, 10% Tet-tested FBS (Atlanta Biologicals), 20 mM HEPES, 2 mM L-glutamine, antibiotic/antimycotic, nonessential amino acids, 500 µg/mL G418, 100 µg/mL hygromycin, and 5 µg/mL blasticidin S at 37 °C in the presence of 5% CO₂.

HEK293A mGlu₂ G₄₁₅ Cell Line Creation. In order to generate a rat mGlu₂ stable cell line to be used for a calcium mobilization assay, HEK293A cells (ATCC) were transfected with mouse G₄₁₅-pCMV6 plasmid (Origene) using Fugene6 (Promega). The cells were selected for G₄₁₅ expression with 1 mg/mL G418. Two weeks after the selection, polyclonal HEK293A G₄₁₅ cells were obtained. The entire coding sequence of rat mGlu₂ was amplified by PCR and cloned into the expression plasmid pIRESpuro3 (Invitrogen). Rat mGlu₂-pIRESpuro3 was transfected into HEK293A G₄₁₅ cells and selected for mGlu₂ expression with 0.6 µg/mL puromycin in the presence of G418. The resulting polyclonal HEK293A mGlu₂ G₄₁₅ cells were then utilized for calcium mobilization assays. Cells were maintained in growth medium containing DMEM, 10% FBS, 20 mM HEPES, 2 mM L-glutamine, antibiotic/antimycotic, nonessential amino acids, 700 µg/mL G418, and 0.6 µg/mL puromycin at 37 °C in the presence of 5% CO₂.

Western Blotting. Western blotting was performed as detailed previously⁵⁸ utilizing 10% polyacrylamide gels and a rabbit polyclonal mGlu_{2/3} antibody (Millipore, catalog no. 06-676) for detection of mGlu₃.

Microsomal Stability In Vitro Assay. Pooled rat liver microsomes (BD Biosciences, no. 452701) were preincubated with test compounds at 37.5 °C for 5 min in the absence of NADPH. The reaction was initiated by addition of NADPH, and the mixture was incubated under the same conditions. The final incubation concentrations were 4 µM test compound, 2 mM NADPH, and 1 mg/mL (total protein) liver microsomes in phosphate buffered saline (PBS) at pH 7.4. One aliquot (100 µL) of the incubation mixture was withdrawn at 15 min time points and combined immediately with 100 µL of ACN/MeOH. After mixing, the sample was centrifuged at approximately 13 000 rpm for 12 min. The supernatant was filtered and transferred into an autosampler vial, and the amount of test compound was quantified using a Shimadzu LCMS 2010EV mass spectrometer. The change of the AUC (area under the curve) of the parent compound as a function of time was used as a measure of microsomal stability. Test compounds were run in duplicate with a positive control.

Plasma Stability In Vitro Assay. A 20 µL aliquot of a 10 mM solution in DMSO of the test compound was added to 2.0 mL of heparinized rat plasma (Lampire, P1-150N) to obtain a 100 µM final solution. The mixture was incubated for 1 h at 37.5 °C. Aliquots of 100 µL were taken at 15 min intervals and diluted with 100 µL of MeOH/ACN. After mixing, the sample was centrifuged at approximately 13 000 rpm for 12 min. The supernatant was filtered and transferred into an autosampler vial, and the amount of test compound was quantified using the Shimadzu LCMS-2010EV system. The change of the AUC of the parent compound as a function of time was used as a measure of plasma stability.

Parallel Artificial Membrane Permeation Assay (PAMPA). A 96-well microtiter plate (Millipore, MSSACCEPTOR) was filled with 300 µL of aqueous buffer solution (in general, phosphate pH 7.2 buffer was used) and covered with a microtiter filterplate (Millipore, MAIPNTR10) to create a sort of sandwich construction. The hydrophobic filter material was impregnated with a 10% solution of polar brain lipid extract in chloroform (Avanti) as the artificial membrane, and the organic solvent was allowed to completely evaporate. Permeation studies were started by the transfer of 150 µL of a 100 µM test compound solution on top of the filter plate. The maximum DMSO content of the stock solutions was <1.5%. In parallel, an equilibrium solution lacking a membrane was prepared using the exact concentrations

and specifications but lacking the membrane. The concentrations of the acceptor and equilibrium solutions were determined using the Shimadzu LCMS-2010EV and AUC methods. The acceptor plate and equilibrium plate concentrations were used to calculate the permeability rate (log *P_e*) of the compounds. The log *P_e* values were calculated using the following equations:

$$\log P_e = \log \left\{ C \left[-\ln \left(1 - \frac{[\text{drug}]_{\text{acceptor}}}{[\text{drug}]_{\text{equilibrium}}} \right) \right] \right\}$$

$$C = \frac{V_D V_A}{(V_D + V_A)(\text{area})(\text{time})}$$

In this equation, *V_D* (cm³) is the donor volume (0.150 cm³), *V_A* (cm³) is the acceptor volume (0.300 cm³), area (cm²) is the accessible filter area (0.168 cm²), and time (s) is the incubation time. Variables [drug]_{acceptor} and [drug]_{equilibrium} are concentrations of the test drug for the sample (acceptor) and reference (equilibrium) solutions in the acceptor compartment.

Behavioral Assessments. Subjects. Male Wistar rats (Charles River Laboratories, Raleigh, NC) weighing 300–350 g at the beginning of each experiment were housed in pairs in standard rat Plexiglas cages with food and water available ad libitum except during food training and the food self-administration experiment (see below). Rats were maintained in a climate-controlled room at 21 °C on a 12 h reverse light/dark cycle, and all experiments were conducted during the dark (i.e., active) phase (7:00 to 19:00 h) of the cycle under dim red lighting. All procedures were conducted in accordance with the guidelines from the National Institutes of Health and the Association for the Assessment and Accreditation of Laboratory Animal Care and were approved by the Institutional Animal Care and Use Committee.

Drugs. Cocaine hydrochloride (National Institute on Drug Abuse, Bethesda, MD) was dissolved in sterile physiological saline and filtered through a 0.22 µm syringe filter (Fisher Scientific, Pittsburgh, PA) for sterilization purposes. **74** was mixed into a 10% EtOH, 1% Tween 80 solution.

Food Training. Details regarding the experimental procedures have been described previously.³⁷ All rats were placed under food restriction (20 g of food/day) and trained during daily 1 h sessions to lever-press for 45 mg food pellets (Research Diets, New Brunswick, NJ) under a fixed ratio 1 reinforcement schedule with a 1 s time-out period (FR1 TO1s). Successful responses were followed by illumination of a cue light for the duration of the time-out period, when lever presses had no consequence. Successful acquisition of food responding, defined as earning 100 pellets during each session, resulted in progression of the training program to FR1 TO10s and FR1 TO20s. Training lasted approximately 5 days.

Cocaine Self-Administration Experiment. After successful acquisition of food training, rats (*n* = 11) were fed ad libitum, surgically prepared with intravenous catheters inserted into the right jugular vein under isoflurane anesthesia (1–1.5% isoflurane/oxygen mixture), and allowed 7 days to recover (see Jin et al. (2010) for details). Rats were then trained to self-administer cocaine under a FR1 TO20s reinforcement schedule during daily 1 h sessions. Each response at the active lever resulted in an intravenous infusion of cocaine (0.5 mg/kg/infusion) over a 2 s period in a volume of 0.05 µL. Rats were trained for approximately 10 days until responding for cocaine stabilized (i.e., >10 infusions/session; <20% variability in number of infusions over three consecutive sessions). After stabilization of responding, rats were administered **74** (0, 10, 20, 40 mg/kg, ip; 3 mL/kg volume; 60 min pretreatment time) according to a within-subjects Latin-square design. At least 4 days elapsed between drug/vehicle injections to re-establish stable self-administration behavior (<20% variability over three consecutive sessions).

Food Self-Administration Experiment. To assess nonspecific actions of **74**, after successful acquisition of food training and stabilization of responding (<20% variability over three consecutive sessions), rats (*n* = 8) were administered **74** (0, 10, 20, 40 mg/kg, ip; 3 mL/kg volume; 60 min pretreatment time) according to a within-subjects

Latin-square design. All test parameters, including the FR1 TO20s reinforcement schedule, were identical to the parameters under which cocaine was self-administered.

Statistical Analyses. The number of cocaine infusions/food pellets earned during test sessions with 74 was calculated as a percentage of the average number of infusions/pellets earned during the prior three baseline sessions. Data were then analyzed with a mixed design analysis of variance (ANOVA) with 74 dose (within-subjects) and self-administration (i.e., cocaine vs food; between-subjects) as factors. Significant effects were further analyzed with Tukey post hoc tests. The level of significance was set at $\alpha = 0.05$.

■ ASSOCIATED CONTENT

■ Supporting Information

Computationally determined plasma–protein binding for 11 compounds and off-target profiling data against a panel of CNS receptors for compound 72. This material is available free of charge via the Internet at <http://pubs.acs.org>.

■ AUTHOR INFORMATION

Corresponding Author

*Phone: 858-646-3100. Fax: 858-795-5225. E-mail: ncosford@sanfordburnham.org

Author Contributions

#R.-P.D. and D.J.S. contributed equally.

Notes

The authors declare no competing financial interest.

■ ACKNOWLEDGMENTS

This work was supported by National Institutes of Health Grant R01 DA023926 to N.D.P.C. and NIDA grant DA011946 to A.M. D.J.S. is a recipient of a National Alliance for Research on Schizophrenia and Depression (NARSAD), Dylan Tauber Young Investigator Award. The binding profile for compound 72 was generously provided by the National Institute of Mental Health's Psychoactive Drug Screening Program, Contract HHSN-271-2008-00025-C (NIMH PDSP).

■ ABBREVIATIONS USED

mGlu₂, metabotropic glutamate receptor subtype 2; PAM, positive allosteric modulator; BINA, 3'-((2-cyclopentyl-6,7-dimethyl-1-oxo-2,3-dihydro-1H-inden-5-yloxy)methyl)-biphenyl-4-carboxylic acid; HTS, high-throughput screening; PK, pharmacokinetic; POC, proof-of-concept; ADME, absorption, distribution, metabolism, excretion; AUC, area under curve; LOQ, limit of quantitation; HEK, human embryonic kidney; GIRK, G protein-coupled inwardly rectifying potassium; PBS, phosphate buffered saline; DMEM, Dulbecco's modified Eagle medium; HEPES, 4-(2-hydroxyethyl)-1-piperazineethanesulfonic acid; FBS, fetal bovine serum

■ REFERENCES

- (1) Marmiroli, P.; Cavaletti, G. The glutamatergic neurotransmission in the central nervous system. *Curr. Med. Chem.* **2012**, *19*, 1269–1276.
- (2) Sheffler, D. J.; Gregory, K. J.; Rook, J. M.; Conn, P. J. Allosteric modulation of metabotropic glutamate receptors. *Adv. Pharmacol.* **2011**, *62*, 37–77.
- (3) Conn, P. J.; Pin, J. P. Pharmacology and functions of metabotropic glutamate receptors. *Annu. Rev. Pharmacol. Toxicol.* **1997**, *37*, 205–237.
- (4) Enz, R. Metabotropic glutamate receptors and interacting proteins: evolving drug targets. *Curr. Drug Targets* **2012**, *13*, 145–156.
- (5) Sheffler, D. J.; Pinkerton, A. B.; Dahl, R.; Markou, A.; Cosford, N. D. Recent progress in the synthesis and characterization of group II

metabotropic glutamate receptor allosteric modulators. *ACS Chem. Neurosci.* **2011**, *2*, 382–393.

(6) Cartmell, J.; Schoepp, D. D. Regulation of neurotransmitter release by metabotropic glutamate receptors. *J. Neurochem.* **2000**, *75*, 889–907.

(7) Durand, D.; Carniglia, L.; Caruso, C.; Lasaga, M. mGlu3 receptor and astrocytes: partners in neuroprotection. *Neuropharmacology* **2013**, *66*, 1–11.

(8) Corti, C.; Battaglia, G.; Molinaro, G.; Riozzi, B.; Pittaluga, A.; Corsi, M.; Mugnaini, M.; Nicoletti, F.; Bruno, V. The use of knock-out mice unravels distinct roles for mGlu2 and mGlu3 metabotropic glutamate receptors in mechanisms of neurodegeneration/neuroprotection. *J. Neurosci.* **2007**, *27*, 8297–8308.

(9) Ohishi, H.; Neki, A.; Mizuno, N. Distribution of a metabotropic glutamate receptor, mGluR2, in the central nervous system of the rat and mouse: an immunohistochemical study with a monoclonal antibody. *Neurosci. Res.* **1998**, *30*, 65–82.

(10) Wright, R. A.; Arnold, M. B.; Wheeler, W. J.; Ornstein, P. L.; Schoepp, D. D. [³H]LY341495 binding to group II metabotropic glutamate receptors in rat brain. *J. Pharmacol. Exp. Ther.* **2001**, *298*, 453–460.

(11) Swanson, C. J.; Bures, M.; Johnson, M. P.; Linden, A. M.; Monn, J. A.; Schoepp, D. D. Metabotropic glutamate receptors as novel targets for anxiety and stress disorders. *Nat. Rev. Drug Discovery* **2005**, *4*, 131–144.

(12) Krystal, J. H.; Mathew, S. J.; D'Souza, D. C.; Garakani, A.; Gunduz-Bruce, H.; Charney, D. S. Potential psychiatric applications of metabotropic glutamate receptor agonists and antagonists. *CNS Drugs* **2010**, *24*, 669–693.

(13) Chaki, S.; Ago, Y.; Palucha-Paniewiera, A.; Matrisciano, F.; Pilc, A. mGlu2/3 and mGlu5 receptors: potential targets for novel antidepressants. *Neuropharmacology* **2013**, *66*, 40–52.

(14) Conn, P. J.; Lindsley, C. W.; Jones, C. K. Activation of metabotropic glutamate receptors as a novel approach for the treatment of schizophrenia. *Trends Pharmacol. Sci.* **2009**, *30*, 25–31.

(15) Sheffler, D. J.; Conn, P. J. Activation of Group II Metabotropic Glutamate Receptors (mGluR2 and mGluR3) as a Novel Approach for Treatment of Schizophrenia. In *Glutamate-Based Therapies for Psychiatric Disorders*; Skolnick, P., Ed.; Birkhäuser: Basel, Switzerland, 2010; pp 101–116.

(16) Kenny, P. J.; Markou, A. The ups and downs of addiction: role of metabotropic glutamate receptors. *Trends Pharmacol. Sci.* **2004**, *25*, 265–272.

(17) Xi, Z. X.; Ramamoorthy, S.; Baker, D. A.; Shen, H.; Samuvel, D. J.; Kalivas, P. W. Modulation of group II metabotropic glutamate receptor signaling by chronic cocaine. *J. Pharmacol. Exp. Ther.* **2002**, *303*, 608–615.

(18) Adewale, A. S.; Platt, D. M.; Spealman, R. D. Pharmacological stimulation of group II metabotropic glutamate receptors reduces cocaine self-administration and cocaine-induced reinstatement of drug seeking in squirrel monkeys. *J. Pharmacol. Exp. Ther.* **2006**, *318*, 922–931.

(19) Aujla, H.; Martin-Fardon, R.; Weiss, F. Rats with extended access to cocaine exhibit increased stress reactivity and sensitivity to the anxiolytic-like effects of the mGluR 2/3 agonist LY379268 during abstinence. *Neuropsychopharmacology* **2008**, *33*, 1818–1826.

(20) Baptista, M. A.; Martin-Fardon, R.; Weiss, F. Preferential effects of the metabotropic glutamate 2/3 receptor agonist LY379268 on conditioned reinstatement versus primary reinforcement: comparison between cocaine and a potent conventional reinforcer. *J. Neurosci.* **2004**, *24*, 4723–4727.

(21) Peters, J.; Kalivas, P. W. The group II metabotropic glutamate receptor agonist, LY379268, inhibits both cocaine- and food-seeking behavior in rats. *Psychopharmacology (Berlin, Ger.)* **2006**, *186*, 143–149.

(22) Xi, Z. X.; Baker, D. A.; Shen, H.; Carson, D. S.; Kalivas, P. W. Group II metabotropic glutamate receptors modulate extracellular glutamate in the nucleus accumbens. *J. Pharmacol. Exp. Ther.* **2002**, *300*, 162–171.

- (23) Flor, P. J.; Battaglia, G.; Nicoletti, F.; Gasparini, F.; Bruno, V. Neuroprotective activity of metabotropic glutamate receptor ligands. *Adv. Exp. Med. Biol.* **2002**, *513*, 197–223.
- (24) Allen, J. W.; Ivanova, S. A.; Fan, L.; Espey, M. G.; Basile, A. S.; Faden, A. I. Group II metabotropic glutamate receptor activation attenuates traumatic neuronal injury and improves neurological recovery after traumatic brain injury. *J. Pharmacol. Exp. Ther.* **1999**, *290*, 112–120.
- (25) Richards, G.; Messer, J.; Faull, R. L.; Stadler, H.; Wichmann, J.; Huguenin, P.; Bohrmann, B.; Mutel, V. Altered distribution of mGlu2 receptors in beta-amyloid-affected brain regions of Alzheimer cases and aged PS2APP mice. *Brain Res.* **2010**, *1363*, 180–190.
- (26) Ahnaou, A.; Dautzenberg, F. M.; Geys, H.; Imogai, H.; Gibelin, A.; Moechars, D.; Steckler, T.; Drinkenburg, W. H. Modulation of group II metabotropic glutamate receptor (mGlu2) elicits common changes in rat and mice sleep–wake architecture. *Eur. J. Pharmacol.* **2009**, *603*, 62–72.
- (27) Monn, J. A.; Valli, M. J.; Massey, S. M.; Hansen, M. M.; Kress, T. J.; Wepsiec, J. P.; Harkness, A. R.; Grutsch, J. L., Jr.; Wright, R. A.; Johnson, B. G.; Andis, S. L.; Kingston, A.; Tomlinson, R.; Lewis, R.; Griffey, K. R.; Tizzano, J. P.; Schoepp, D. D. Synthesis, pharmacological characterization, and molecular modeling of heterobicyclic amino acids related to (+)-2-aminobicyclo[3.1.0]hexane-2,6-dicarboxylic acid (LY354740): identification of two new potent, selective, and systemically active agonists for group II metabotropic glutamate receptors. *J. Med. Chem.* **1999**, *42*, 1027–1040.
- (28) Dominguez, C.; Prieto, L.; Valli, M. J.; Massey, S. M.; Bures, M.; Wright, R. A.; Johnson, B. G.; Andis, S. L.; Kingston, A.; Schoepp, D. D.; Monn, J. A. Methyl substitution of 2-aminobicyclo[3.1.0]hexane 2,6-dicarboxylate (LY354740) determines functional activity at metabotropic glutamate receptors: identification of a subtype selective mGlu2 receptor agonist. *J. Med. Chem.* **2005**, *48*, 3605–3612.
- (29) Hanna, L.; Ceolin, L.; Lucas, S.; Monn, J.; Johnson, B.; Collingridge, G.; Bortolotto, Z.; Lodge, D. Differentiating the roles of mGlu2 and mGlu3 receptors using LY541850, an mGlu2 agonist/mGlu3 antagonist. *Neuropharmacology* **2013**, *66*, 114–121.
- (30) Anwyl, R. Metabotropic glutamate receptors: electrophysiological properties and role in plasticity. *Brain Res. Rev.* **1999**, *29*, 83–120.
- (31) Cartmell, J.; Monn, J. A.; Schoepp, D. D. The metabotropic glutamate 2/3 receptor agonists LY354740 and LY379268 selectively attenuate phencyclidine versus D-amphetamine motor behaviors in rats. *J. Pharmacol. Exp. Ther.* **1999**, *291*, 161–170.
- (32) Wieronska, J. M.; Stachowicz, K.; Branski, P.; Palucha-Poniewiera, A.; Pilc, A. On the mechanism of anti-hyperthermic effects of LY379268 and LY487379, group II mGlu receptors activators, in the stress-induced hyperthermia in singly housed mice. *Neuropharmacology* **2012**, *62*, 322–331.
- (33) Galici, R.; Jones, C. K.; Hemstapat, K.; Nong, Y.; Echemendia, N. G.; Williams, L. C.; de Paulis, T.; Conn, P. J. Biphenyl-indanone A, a positive allosteric modulator of the metabotropic glutamate receptor subtype 2, has antipsychotic- and anxiolytic-like effects in mice. *J. Pharmacol. Exp. Ther.* **2006**, *318*, 173–185.
- (34) Reiner, A.; Lafferty, D. C.; Wang, H. B.; Del Mar, N.; Deng, Y. P. The group 2 metabotropic glutamate receptor agonist LY379268 rescues neuronal, neurochemical and motor abnormalities in R6/2 Huntington's disease mice. *Neurobiol. Dis.* **2012**, *47*, 75–91.
- (35) Reiner, A.; Wang, H. B.; Del Mar, N.; Sakata, K.; Yoo, W.; Deng, Y. P. BDNF may play a differential role in the protective effect of the mGluR2/3 agonist LY379268 on striatal projection neurons in R6/2 Huntington's disease mice. *Brain Res.* **2012**, *1473*, 161–172.
- (36) Schiefer, J.; Sprunken, A.; Puls, C.; Luesse, H. G.; Milkereit, A.; Milkereit, E.; Johann, V.; Kosinski, C. M. The metabotropic glutamate receptor 5 antagonist MPEP and the mGluR2 agonist LY379268 modify disease progression in a transgenic mouse model of Huntington's disease. *Brain Res.* **2004**, *1019*, 246–254.
- (37) Jin, X.; Semenova, S.; Yang, L.; Ardecky, R.; Sheffler, D. J.; Dahl, R.; Conn, P. J.; Cosford, N. D.; Markou, A. The mGluR2 positive allosteric modulator BINA decreases cocaine self-administration and cue-induced cocaine-seeking and counteracts cocaine-induced enhancement of brain reward function in rats. *Neuropsychopharmacology* **2010**, *35*, 2021–2036.
- (38) Bossert, J. M.; Poles, G. C.; Sheffler-Collins, S. I.; Ghitza, U. E. The mGluR2/3 agonist LY379268 attenuates context- and discrete cue-induced reinstatement of sucrose seeking but not sucrose self-administration in rats. *Behav. Brain Res.* **2006**, *173*, 148–152.
- (39) Cacciola, J.; Empfield, J.; Folmer, J.; Hunter, A. M.; Throner, S. Metabotropic glutamate receptor isoxazole ligands and their use as potentiators 286. U.S. Patent 7,790,760, September 7, 2010.
- (40) Pinkerton, A. B.; Cube, R. V.; Hutchinson, J. H.; Rowe, B. A.; Schaffhauser, H.; Zhao, X.; Daggett, L. P.; Vernier, J. M. Allosteric potentiators of the metabotropic glutamate receptor 2 (mGlu2). Part 1: Identification and synthesis of phenyl-tetrazolyl acetophenones. *Bioorg. Med. Chem. Lett.* **2004**, *14*, 5329–5332.
- (41) Pinkerton, A. B.; Cube, R. V.; Hutchinson, J. H.; James, J. K.; Gardner, M. F.; Rowe, B. A.; Schaffhauser, H.; Rodriguez, D. E.; Campbell, U. C.; Daggett, L. P.; Vernier, J. M. Allosteric potentiators of the metabotropic glutamate receptor 2 (mGlu2). Part 3: Identification and biological activity of indanone containing mGlu2 receptor potentiators. *Bioorg. Med. Chem. Lett.* **2005**, *15*, 1565–1571.
- (42) Johnson, M. P.; Baez, M.; Jagdmann, G. E., Jr.; Britton, T. C.; Large, T. H.; Callagaro, D. O.; Tizzano, J. P.; Monn, J. A.; Schoepp, D. D. Discovery of allosteric potentiators for the metabotropic glutamate 2 receptor: synthesis and subtype selectivity of N-(4-(2-methoxyphenoxy)phenyl)-N-(2,2,2-trifluoroethylsulfonyl)pyrid-3-yl-methylamine. *J. Med. Chem.* **2003**, *46*, 3189–3192.
- (43) Pinkerton, A. B.; Vernier, J. M.; Schaffhauser, H.; Rowe, B. A.; Campbell, U. C.; Rodriguez, D. E.; Lorrain, D. S.; Bacceti, C. S.; Daggett, L. P.; Bristow, L. J. Phenyl-tetrazolyl acetophenones: discovery of positive allosteric potentiators for the metabotropic glutamate 2 receptor. *J. Med. Chem.* **2004**, *47*, 4595–4599.
- (44) Govek, S. P.; Bonnefous, C.; Hutchinson, J. H.; Kamenecka, T.; McQuiston, J.; Pracitto, R.; Zhao, L. X.; Gardner, M. F.; James, J. K.; Daggett, L. P.; Rowe, B. A.; Schaffhauser, H.; Bristow, L. J.; Campbell, U. C.; Rodriguez, D. E.; Vernier, J. M. Benzazoles as allosteric potentiators of metabotropic glutamate receptor 2 (mGluR2): efficacy in an animal model for schizophrenia. *Bioorg. Med. Chem. Lett.* **2005**, *15*, 4068–4072.
- (45) Duplantier, A. J.; Efremov, I.; Candler, J.; Doran, A. C.; Ganong, A. H.; Haas, J. A.; Hanks, A. N.; Kraus, K. G.; Lazzaro, J. T., Jr.; Lu, J.; Maklad, N.; McCarthy, S. A.; O'Sullivan, T. J.; Rogers, B. N.; Siuciak, J. A.; Spracklin, D. K.; Zhang, L. 3-Benzyl-1,3-oxazolidin-2-ones as mGluR2 positive allosteric modulators: hit-to lead and lead optimization. *Bioorg. Med. Chem. Lett.* **2009**, *19*, 2524–2529.
- (46) Tresadern, G.; Cid, J. M.; Macdonald, G. J.; Vega, J. A.; de Lucas, A. I.; Garcia, A.; Matesanz, E.; Linares, M. L.; Oehlich, D.; Lavreysen, H.; Biesmans, I.; Trabanco, A. A. Scaffold hopping from pyridones to imidazo[1,2-a]pyridines. New positive allosteric modulators of metabotropic glutamate 2 receptor. *Bioorg. Med. Chem. Lett.* **2010**, *20*, 175–179.
- (47) Melancon, B. J.; Hopkins, C. R.; Wood, M. R.; Emmitte, K. A.; Niswender, C. M.; Christopoulos, A.; Conn, P. J.; Lindsley, C. W. Allosteric modulation of seven transmembrane spanning receptors: theory, practice, and opportunities for central nervous system drug discovery. *J. Med. Chem.* **2012**, *55*, 1445–1464.
- (48) Dhanya, R. P.; Sidique, S.; Sheffler, D. J.; Nickols, H. H.; Herath, A.; Yang, L.; Dahl, R.; Ardecky, R.; Semenova, S.; Markou, A.; Conn, P. J.; Cosford, N. D. Design and synthesis of an orally active metabotropic glutamate receptor subtype-2 (mGluR2) positive allosteric modulator (PAM) that decreases cocaine self-administration in rats. *J. Med. Chem.* **2011**, *54*, 342–353.
- (49) Sidique, S.; Dhanya, R. P.; Sheffler, D. J.; Nickols, H. H.; Yang, L.; Dahl, R.; Mangravita-Novo, A.; Smith, L. H.; D'Souza, M. S.; Semenova, S.; Conn, P. J.; Markou, A.; Cosford, N. D. Orally active metabotropic glutamate subtype 2 receptor positive allosteric modulators: structure–activity relationships and assessment in a rat model of nicotine dependence. *J. Med. Chem.* **2012**, *55*, 9434–9445.

(50) Schann, S.; Mayer, S.; Franchet, C.; Frauli, M.; Steinberg, E.; Thomas, M.; Baron, L.; Neuville, P. Chemical switch of a metabotropic glutamate receptor 2 silent allosteric modulator into dual metabotropic glutamate receptor 2/3 negative/positive allosteric modulators. *J. Med. Chem.* **2010**, *53*, 8775–8779.

(51) Cube, R. V.; Vernier, J. M.; Hutchinson, J. H.; Gardner, M. F.; James, J. K.; Rowe, B. A.; Schaffhauser, H.; Daggett, L.; Pinkerton, A. B. 3-(2-Ethoxy-4-{4-[3-hydroxy-2-methyl-4-(3-methylbutanoyl)-phenoxy]butoxy}phenyl)propanoic acid: a brain penetrant allosteric potentiator at the metabotropic glutamate receptor 2 (mGluR2). *Bioorg. Med. Chem. Lett.* **2005**, *15*, 2389–2393.

(52) Fell, M. J.; Witkin, J. M.; Falcone, J. F.; Katner, J. S.; Perry, K. W.; Hart, J.; Rorick-Kehn, L.; Overshiner, C. D.; Rasmussen, K.; Chaney, S. F.; Benvenista, M. J.; Li, X.; Marlow, D. L.; Thompson, L. K.; Luecke, S. K.; Wafford, K. A.; Seidel, W. F.; Edgar, D. M.; Quets, A. T.; Felder, C. C.; Wang, X.; Heinz, B. A.; Nikolayev, A.; Kuo, M. S.; Mayhugh, D.; Khilevich, A.; Zhang, D.; Ebert, P. J.; Eckstein, J. A.; Ackermann, B. L.; Swanson, S. P.; Catlow, J. T.; Dean, R. A.; Jackson, K.; Tauscher-Wisniewski, S.; Marek, G. J.; Schkeryantz, J. M.; Svensson, K. A. N-(4-((2-(Trifluoromethyl)-3-hydroxy-4-(isobutyryl)-phenoxy)methyl)benzyl)-1-methyl-1H-imidazole-4-carboxamide (THIIC), a novel metabotropic glutamate 2 potentiator with potential anxiolytic/antidepressant properties: in vivo profiling suggests a link between behavioral and central nervous system neurochemical changes. *J. Pharmacol. Exp. Ther.* **2011**, *336*, 165–177.

(53) Liechti, M. E.; Lhuillier, L.; Kaupmann, K.; Markou, A. Metabotropic glutamate 2/3 receptors in the ventral tegmental area and the nucleus accumbens shell are involved in behaviors relating to nicotine dependence. *J. Neurosci.* **2007**, *27*, 9077–9085.

(54) Morishima, Y.; Miyakawa, T.; Furuyashiki, T.; Tanaka, Y.; Mizuma, H.; Nakanishi, S. Enhanced cocaine responsiveness and impaired motor coordination in metabotropic glutamate receptor subtype 2 knockout mice. *Proc. Natl. Acad. Sci. U.S.A.* **2005**, *102*, 4170–4175.

(55) Niswender, C. M.; Johnson, K. A.; Luo, Q.; Ayala, J. E.; Kim, C.; Conn, P. J.; Weaver, C. D. A novel assay of Gi/o-linked G protein-coupled receptor coupling to potassium channels provides new insights into the pharmacology of the group III metabotropic glutamate receptors. *Mol. Pharmacol.* **2008**, *73*, 1213–1224.

(56) Hemstapat, K.; de Paulis, T.; Chen, Y.; Brady, A. E.; Grover, V. K.; Alagille, D.; Tamagnan, G. D.; Conn, P. J. A novel class of positive allosteric modulators of metabotropic glutamate receptor subtype 1 interact with a site distinct from that of negative allosteric modulators. *Mol. Pharmacol.* **2006**, *70*, 616–626.

(57) Engers, D. W.; Niswender, C. M.; Weaver, C. D.; Jadhav, S.; Menon, U. N.; Zamorano, R.; Conn, P. J.; Lindsley, C. W.; Hopkins, C. R. Synthesis and evaluation of a series of heterobiaryl amides that are centrally penetrant metabotropic glutamate receptor 4 (mGluR4) positive allosteric modulators (PAMs). *J. Med. Chem.* **2009**, *52*, 4115–4118.

(58) Sheffler, D. J.; Conn, P. J. Activation of Group II Metabotropic Glutamate Receptors (mGluR2 and mGluR3) as a Novel Approach for Treatment of Schizophrenia. In *Glutamate-Based Therapies for Psychiatric Disorders*; Skolnick, P., Ed.; Birkhäuser: Basel, Switzerland, 2010; pp 101–116.